

---

# 4

---

## MICROENGINEERED POLYMER- AND CERAMIC-BASED BIOMATERIAL SCAFFOLDS: A TOPICAL REVIEW ON DESIGN, PROCESSING, AND BIOCOMPATIBILITY PROPERTIES

GARIMA TRIPATHI<sup>1</sup> AND BIKRAMJIT BASU<sup>2</sup>

<sup>1</sup> *Laboratory for Biomaterials, Department of Material Science and Engineering, Indian Institute of Technology, Kanpur, India*

<sup>2</sup> *Laboratory for Biomaterials, Materials Research Center, Indian Institute of Science, Bangalore, India*

### 4.1 INTRODUCTION

Biomaterials are a class of engineering materials that can be used in tissue replacements, reconstructions, and regeneration without any long-term adverse effect. The development of biomaterials and manufacturing techniques broadened the diversity of applications for various biocompatible materials. A synthetic material or processed natural material is engineered to treat or replace any component or function of a biological organism while in continuous or intermittent contact with biological cells or tissues. Any natural or synthetic material complying with this definition is broadly classified as a biomaterial. In a nutshell, “A biomaterial is a substance that has been engineered to take a form which, alone or as part of a complex system, is used to direct, by control of interactions with components of living systems, the course of any therapeutic or diagnostic procedure, in human or veterinary medicine”.<sup>1</sup> However, in this regard, biocompatibility is of paramount

---

*Micro and Nanotechnologies in Engineering Stem Cells and Tissues*, First Edition. Edited by Murugan Ramalingam, Esmail Jabbari, Seeram Ramakrishna, and Ali Khademhosseini.

© 2013 by The Institute of Electrical and Electronics Engineers, Inc. Published 2013 by John Wiley & Sons, Inc.

importance because debatable safety of the biomaterial may render its application questionable. As defined by David Williams, “Biocompatibility refers to the ability of a biomaterial to perform its desired function with respect to a medical therapy, without eliciting any undesirable local or systemic effects in the recipient or beneficiary of that therapy, but generating the most appropriate beneficial cellular or tissue response in that specific situation, and optimizing the clinically relevant performance of that therapy.”<sup>2</sup>

Depending on the host response and biocompatibility, biomaterials can be typically classified under three categories<sup>3</sup>:

1. *Bioinert or biotolerant* materials, which, although biocompatible, fail to induce interfacial biological bond between natural bone and synthetic implant.
2. *Bioactive* materials, which are biocompatible and can easily attach with the body tissues, forming chemical and biological bond at an early stage in the postimplantation period.
3. *Bioresorbable* materials, which are gradually resorbed and are replaced by new tissues *in vivo*.

As mentioned earlier, a biomaterial must be obligatorily biocompatible (i.e., it must not elude unresolved inflammatory response or demonstrate immunogenicity or cytotoxicity). Additionally, the biomaterial scaffold should be mechanically strong enough, so as not to collapse during handling and the postimplant activities of the patient. Also, tissue scaffolds must be easily sterilizable to avert chances of infection.<sup>4</sup> A further requirement for a scaffold, particularly in hard tissue engineering, should have tailorable interconnected porosity to direct the cells to grow into desired physical form and boost vascularization of the ingrown tissue. In fact, a typical porosity of 90% and a minimum pore diameter of 100  $\mu\text{m}$  are highly desired for cell penetration and proper vascularization of the ingrown tissue.<sup>5-7</sup> Furthermore, scalability, near-net-shape fabrications are highly desirable for cost-effective large-scale production of scaffold materials.

For an immensely complicated system such as the human body, amalgamating the biological and structural properties of a tissue into a biomaterial to engineer germane scaffolds presents a mammoth challenging task. It must be remembered that biomaterials are not subservient vehicles for introduction of cells into the diseased spot whatsoever, but they must be equally proficient in nurturing the endogenous progenitor cells functionally.

The use of materials as part of surgical implant is not new. More specifically, biomaterials in the form of sutures, bone plates, joint replacements, ligaments, and vascular grafts and medical devices such as pacemakers, biosensors, artificial hearts, and blood tubes are widely used to replace or restore the function of traumatized or degenerated tissues or organs, assist in healing, improve function, correct abnormalities, and thus improve the quality of life of the patients. The substitution of bone parts in the body has been done since the pre-Christian era. By the middle of 19th century, medical science attempted to repair body parts with synthetic materials.

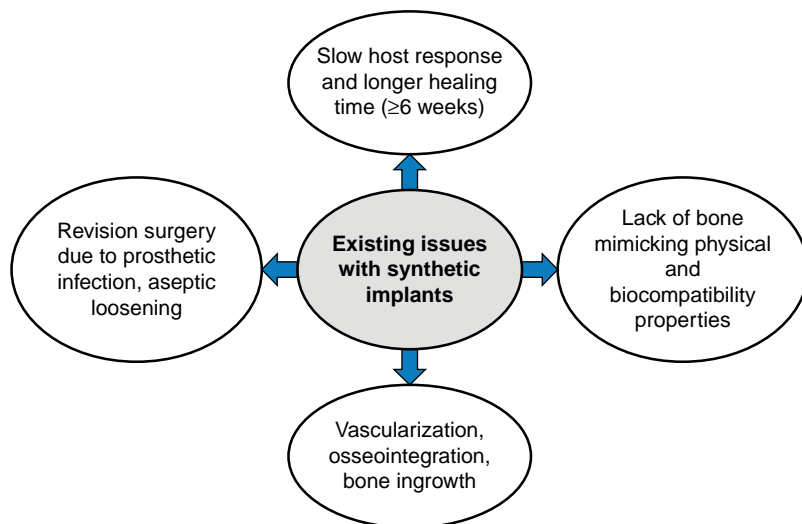


**FIGURE 4.1** Schematic summarizing existing issues with synthetic implants. Adapted from Ref. [20], with permission from John Wiley and Sons.

In 1880, Gluck<sup>8</sup> used ivory prosthesis as implants in the body. In 1902, gold was used in capsule form interposing between the articular heads of an implant.<sup>9</sup> This was a big success, which leads to more study on chemically inert and stable materials. In 1972, Boutin started to study on ceramics such as alumina and zirconia, which did not have biological drawback and were considered everlasting.<sup>10</sup> But both of these ceramics were inert, so implantation was performed without cement anchorage to the tissue. This led to implants loosening very quickly. Such loosening leads to clinical failure, including fracture of the implant or the bone adjacent to the implant. Figure 4.1 summarizes the various existing issues with the synthetic implants such as host response, bone ingrowth, biocompatibility properties, and so on. To improve this unpromising outlook, biologically active or bioactive materials were developed, such as bioglass and hydroxyapatite (HA) by Hench<sup>11</sup> and Jarcho,<sup>12</sup> respectively.

Broadly, all biomaterials are being developed to attain a balance between the physical properties of the replaced tissues and the biochemical effects of the material on the tissue. A summary of the combination of aspects related to processing as well as biological properties to be considered while developing bone analogue materials are provided in Figure 4.2. Despite significant research on biomaterials,<sup>13–19</sup> it has been realized that synthetic materials cannot mimic the extremely complex structure of bone in all aspects and the important disadvantage of synthetic biomaterial is that they cannot repair themselves as living bone does.<sup>20</sup> In addition, the scaffolding offers the opportunity to introduce growth factors into the body. The highly porous materials that are used for scaffolding can be modified with biomolecules, which enhance the ability of the cells to migrate and grow. In this way, the scaffolding does not function simply as a physical structure but instead triggers the proliferation of

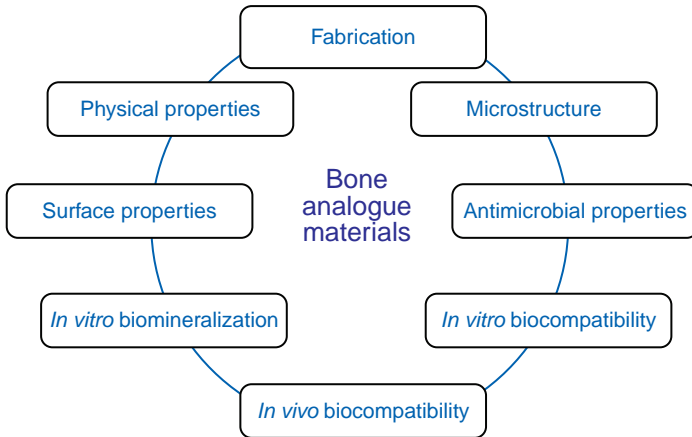


**FIGURE 4.2** Schematic illustrating various approaches or issues to be critically considered while developing bone analogue materials. Adapted from Ref. [20], with permission from John Wiley and Sons.

cells and encourages the surroundings essential for tissue repair. Another approach of tissue engineering is to work with the body’s tissues *in vitro*. In this approach, a small sample of cells is taken from the body, usually with a needle, and then the cells are grown in great number in a laboratory (Fig. 4.3).<sup>21</sup> They may still be grown over scaffolding to give them the necessary shape. These tissues can then be transplanted back into the body.

A summary of the combination of aspects related to fabrication as well as physical and biological properties of bone analogue materials is given in Figure 4.4. As far as the fabrication and microstructure are concerned, there is a wide range of processing techniques, which provide variation in microstructure. Among the physical properties, strength, modulus, and toughness are the important parameters. The physical properties are related to the microstructure as well the surface properties of the as-processed material. Surface properties include the surface roughness, porosity,

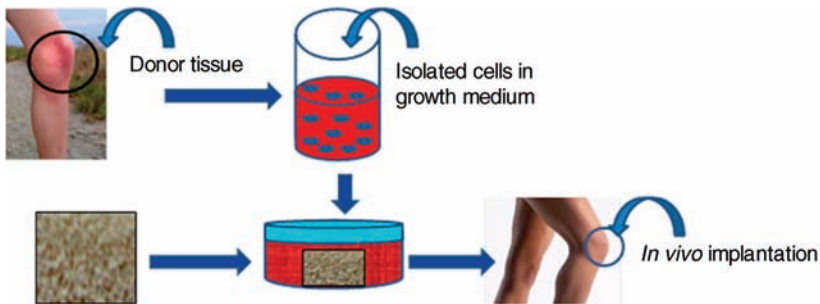


**FIGURE 4.3** Schematic showing the tissue-engineering concept using a hypothetical example of implantation of scaffold for leg regeneration. Adapted from Ref. [20], with permission from John Wiley and Sons.

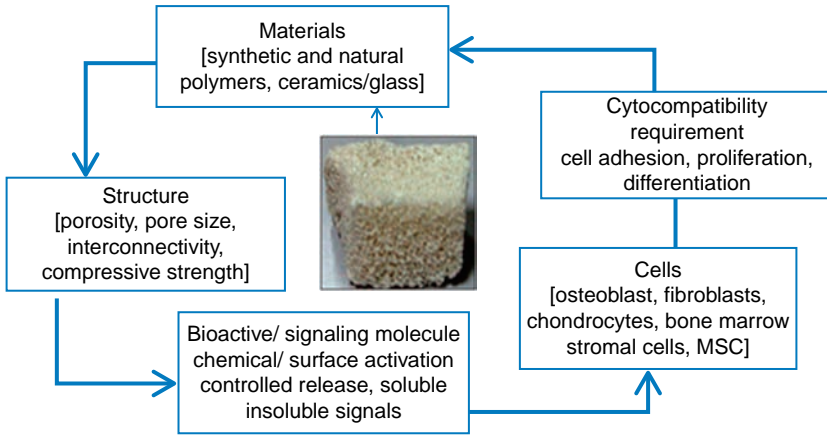


**FIGURE 4.4** Property requirements for porous scaffolds for bone tissue engineering. MSC, mesenchymal stem cell. Idea adapted from Ref. 53.

charge, and wettability of the material. Antimicrobial properties of a material render resistance toward the bacterial adhesion and therefore the prosthetic infection. Among biological properties, cellular functionality and cell fate process are to be considered. *In vivo* osseointegration is important for hard tissue replacement applications. It is impossible to optimize the array of properties in a unique material composition. Therefore, a synergistic approach to combining various properties in designed composite materials is a possible solution.

Considering the options for various functional artificial biomaterials, the choice has to be made among metals, polymers, and ceramics. Each group exhibits some *a priori* advantages and drawbacks. Ceramics, for instance, are the most biocompatible materials and can be obtained with biostable, bioactive, or bioresorbable properties. They are well known for their good bioactivity, corrosion resistance, high compression strength, and high hardness. At the same time, they also have some drawbacks such as low fracture toughness and high stiffness. The elastic modulus of ceramics is at least an order of magnitude higher than those of hard tissues. Therefore, one of the major problems in orthopedic surgery is the significant difference between the stiffness of the bone and ceramic implants. As a result, the bone is insufficiently loaded compared with the implant; this phenomenon is known as “stress shielding” or stress protection. On the other hand, metals exhibit problems of corrosion and toxicity, but their mechanical strength and toughness are superior to those of ceramics. Polymers offer many possibilities depending on their chemical composition and structure (e.g., biodegradability degree, hydrophilic–hydrophobic ratio, toughness or flexibility), but very few have shown good bioactive properties to ensure implant osteointegration. Therefore, it is important to reach the best compromise possible, and it is quite usual to use two or more types of materials in the same implant. Polymer–ceramic or polymer–inorganic composites could be the alternative way to overcome many shortcomings, as mentioned earlier.

This chapter is structured into following sections. After the introductory section and general overview of biomaterials, the section on dense HA versus porous HA scaffold emphasizes the necessity of porosity for better *in vitro* and *in vivo* properties. The section on property requirements of porous scaffold describes the fundamental aspects of these essential requirements. After this, the design criteria and critical issues with porous scaffolds for bone tissue engineering are discussed. The next section provides an exculpation of porous scaffolds. Section 4.5 summarizes the requirement of porosity and future application. A detailed discussion follows on various fabrication processes for porous scaffolds, including a brief discussion on the advantages and disadvantages of typical processing routes in Section 4.6. Section 4.7 provides an overview of physicochemical property evaluation of porous scaffold. The biological property evaluation in terms of *in vitro* and *in vivo* assay results reported by various researchers is summarized in Section 4.8. This chapter closes with the mention of some outstanding issues related to future research on porous scaffold.

## 4.2 DENSE HYDROXYAPATITE VERSUS POROUS HYDROXYAPATITE SCAFFOLD

The inorganic phase of our bones is apatite, more commonly known as hydroxyapatite ( $\text{Ca}_{10}(\text{PO}_4)_6(\text{OH})_2$ ).<sup>22</sup> Its structure has the special ability to accommodate several different ions in its three sublattices.<sup>23,24</sup> Bone apatites could be considered as basic calcium phosphates. To work for potential hard tissue replacement solutions, it is essential to know the bone regeneration process. Wolf's law dictates that the bone remodels itself as a function of forces acting on it, hence preserving its shape and density.<sup>25</sup> The mechanical loads of stress, compression, flex, and torsion in bones and the interstitial fluid contained in them generate stresses and deformations at the microscopical level, which in turn stimulate the bone cells.<sup>26</sup>

Hydroxyapatite [ $\text{Ca}_{10}(\text{PO}_4)_6(\text{OH})_2$ ] is one of the most widely studied inorganic material and is well known for its biocompatibility, bioactivity, high osteoconductivity, and relatively high strength and modulus.<sup>27,28</sup> HA is the most important bioceramic materials for its unique bioactivity and stability. Unlike other calcium phosphates, HA does not break down under physiological conditions. In fact, it is thermodynamically stable at physiological pH and actively takes part in bone bonding, forming strong chemical bonds with surrounding bone. This property has been exploited for rapid bone repair after major trauma or surgery. Although its mechanical properties have been found to be unsuitable for load-bearing applications such as orthopedics, it is used as a coating on load-bearing implant materials such as titanium and titanium alloys or composites with other materials.

Porous HA ceramics have found enormous use in biomedical applications, including bone tissue regeneration, cell proliferation, and drug delivery. HA with controlled porosity is analogous to the natural ceramic in human bone. It is bioactive in the sense that interfacial bonds can develop between HA and the living tissues, leading to enhanced mechanical strength of the overall structure. However, the lower

**TABLE 4.1 Pore Size Distribution for an Ideal Scaffold in Bone Tissue Engineering Applications**

Pore Size	Biological Function
<1 $\mu\text{m}$	Protein interaction; responsible for bioactivity
1–20 $\mu\text{m}$	Cell attachment; their orientation of cellular growth (directionally)
100–1000 $\mu\text{m}$	Cellular growth and bone ingrowth
>1000 $\mu\text{m}$	Shape and functionality of implant

Idea adapted from Ref. [29].

mechanical strength of pure HA has hampered its use as a bone implant material because of conflicting requirements of porosity and strength.

Porous HA exhibits strong bonding to the bone; the pores provide a mechanical interlock leading to a firm fixation of the material. Bone tissue grows well through the pores, thus increasing strength of the HA implant *in vivo*. The ideal bone substitute material should form a secure bond with the tissues by encouraging new cells to grow and penetrate. New tissue and bone formation can easily take place on osteophilic and porous implant and also helps to prevent loosening and movement of the implant. When pore sizes exceed 100  $\mu\text{m}$ , the bone grows through the channels of interconnected surface pores, thus maintaining the bone's vascularity and viability. The application of implant depends on the pore size, as summarized in Table 4.1.<sup>29</sup> Because porous HA is more resorbable and more osteoconductive than dense HA, there is an increasing interest in the development of synthetic porous HA bone replacement material for the filling of both load-bearing and nonload-bearing osseous defects. In terms of simulating the human bone structure, porous HA scaffold has a large surface area, which is beneficial for adhesion of biological cells and growth of new bone phase.

### 4.3 PROPERTY REQUIREMENT OF POROUS SCAFFOLD

Scaffold properties depend primarily on the nature of the biomaterial and the fabrication process. The scaffolds are based on various materials, such as metals, ceramics, glass, chemically synthesized polymers, natural polymers, and combinations of these materials to form composites. The properties and requirements for scaffolds in bone tissue engineering have been extensively reviewed; recent examples include aspects of degradation,<sup>30–33</sup> mechanical properties,<sup>34–38</sup> cytokine delivery,<sup>39–43</sup> and combinations of scaffolds and cells.<sup>44,45</sup>

Porosity is defined as the percentage of void space in a solid,<sup>46</sup> and it is a morphological property, independent of the material. Pores are necessary for bone tissue formation because they allow migration and proliferation of osteoblasts and mesenchymal cells as well as vascularization.<sup>47</sup> In addition, a porous surface improves mechanical interlocking between the implant biomaterial and the surrounding natural bone, providing greater mechanical stability at the critical interface.<sup>48</sup> The most common techniques used to create porosity in a biomaterial are salt

leaching, gas foaming, phase separation, freeze-drying, and sintering, depending on the scaffold material. The minimum pore size required to regenerate mineralized bone is generally considered to be  $\sim 100 \mu\text{m}$  according to the study by Hulbert et al., and this is on the basis of implantation experiments on calcium aluminate cylindrical pellets with 46% porosity in dog femurs.<sup>49</sup> Whereas large pores (100–150 and 150–200  $\mu\text{m}$ ) showed substantial bone ingrowth, smaller pores (75–100  $\mu\text{m}$ ) resulted in ingrowth of unmineralized osteoid tissue. Smaller pores (10–44 and 44–75  $\mu\text{m}$ ) were penetrated only by fibrous tissue. These results were correlated with normal haversian systems that reach an approximate diameter of 100–200  $\mu\text{m}$ . In a different study, titanium plates with four different pore sizes (50, 75, 100, and 125  $\mu\text{m}$ ) were tested in rabbit femoral defects under nonload-bearing conditions.<sup>50</sup> Bone ingrowth was similar in all the pore sizes, suggesting that 100  $\mu\text{m}$  may not be the critical pore size for nonload-bearing conditions.

Scaffold materials can be synthetic or biologic and degradable or nondegradable, depending on the intended use.<sup>51</sup> Various scaffolds can be categorized into different types in terms of their structural, chemical, and biological characteristics (e.g., ceramics, glasses, polymers). Naturally occurring polymers, synthetic biodegradable, and synthetic nonbiodegradable polymers are the main types of polymers used as biomaterials. It is known that the properties of polymers depend on the composition, structure, and arrangement of their constituent macromolecules.

Scaffolds for bone tissue engineering are subjected to many interlinked and often opposing biological and structural requirements. A major hurdle in the design of scaffolds is that most of the materials are either mechanically strong or bioinert, while degradable materials tend to be mechanically weak.<sup>52</sup> Hence, the fabrication of composites comprising biodegradable polymers and ceramics becomes a suitable option to fulfill the requirements of bioactivity, degradability, and mechanical competence. The desired features of a scaffold, such as interconnectivity, pore size and curvature, and surface roughness directly influence cellular responses, and they also control the degree of nutrient delivery, penetration depth of cells, and metabolic waste removal.<sup>53</sup> The design criteria and critical issues with porous scaffolds for bone tissue engineering are summarized in Figures 4.4 and 4.5.

It is important to meet some criteria while developing the porous scaffold to fulfill the requirements of bone tissue engineering (Figs. 4.5 and 4.6). The property requirements include (1) it must be biocompatible, which enables the cell growth, their attachment to surface, and proliferation; (2) the material should induce strong bone bonding, resulting in osteoconduction and osteoinduction; (3) the rate of new tissue formation and biodegradability should match with each other; (4) the mechanical strength of the scaffolds should be adequate enough to provide mechanical constancy in load-bearing sites before regeneration of new tissue; and (5) porous structure and pore size should be more than 100  $\mu\text{m}$  for cell penetration, tissue ingrowth, and vascularization (see also Table 4.1).<sup>29</sup> As named, porosity is an important factor to allow cells to migrate via pores. The interconnected pores allow cells to migrate in multiple directions under *in vitro* and *in vivo* conditions.



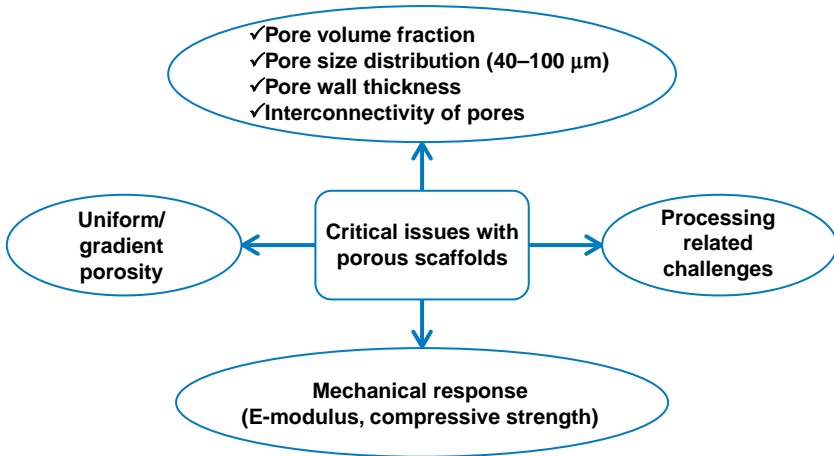


**FIGURE 4.5** Critical issues with porous scaffold for bone tissue engineering.

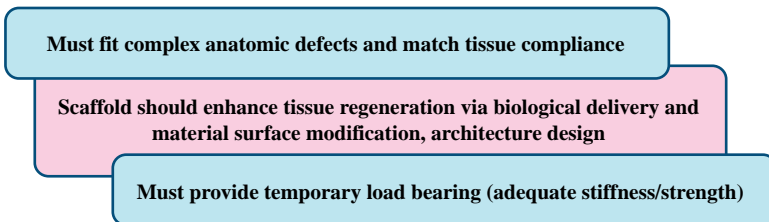


**FIGURE 4.6** Essential requirements of porous scaffolds.

## 4.4 DESIGN CRITERIA AND CRITICAL ISSUES WITH POROUS SCAFFOLDS FOR BONE TISSUE ENGINEERING

### 4.4.1 Cytocompatibility

The most important characteristic feature is compatibility of the implant or porous scaffold with biological cells or tissue. The material should not only be cytocompatible but also foster cell attachment, differentiation, and proliferation. The cellular functionality on porous scaffolds is cell-type dependent, and normally, *in vitro* cell culture assay is performed using osteoblast-like cells or fibroblast-like cell proliferation and adhesion behavior. Also, cell viability in terms of metabolically active cells is measured using a number of assays such as MTT, LDH, and so on. Similarly, the cell differentiation behavior is investigated using an ALP or osteocalcin assay.

#### 4.4.2 Osteoconductivity

According to Wilson-Hench,<sup>54</sup> osteoconduction is the process by which bone is directed so as to conform to a material's surface. However, Glantz<sup>55</sup> has pointed out that this way of looking at bone conduction is somewhat restricted because the original definition bears little or no relation to biomaterials. Osteoconductivity essentially indicates the lack of fibrous tissue encapsulation but also reflects on the possibility of formation of a strong bond between the scaffold and host bone.

#### 4.4.3 Porous Structure

Pores are routinely created in scaffolds to promote three-dimensional (3D) tissue growth, nutrient diffusion, and vascularization. The size of pores must be large enough to allow the circumferential attachment of cells yet small enough to encourage migration and proliferation. The scaffold should have an interconnected porous structure with porosity of more than 90% and pore sizes between 100 and 500  $\mu\text{m}$ , which would be helpful for cell penetration, tissue ingrowth, vascularization, and nutrient delivery.

#### 4.4.4 Mechanical Properties

The mechanical strength of the scaffold should be sufficient to provide mechanical stability to constructs in load-bearing sites before synthesis of new extracellular matrix by cells. The scaffolds should have enough compressive strength, depending on the intended site of application.

#### 4.4.5 Biodegradability

The composition of the material, combined with the porous structure of the scaffold, should lead to biodegradation *in vivo* at rates appropriate to tissue regeneration. Cell transplantation using biodegradable polymer scaffolds offers the possibility to create completely natural new tissue and replace organ function. Tissue-inducing biodegradable polymers can also be used to regenerate certain tissues without the need for *in vitro* cell culture. Also, the biodegradable polymers play an important role in organ regeneration as temporary substrates to transplanted cells, which allow cell attachment, growth, and retention of differentiated function.

#### 4.4.6 Fabrication

The material should possess the ability to be fabricated into irregular shapes of scaffolds, which could match with the defects in bone of individual patient. The synthesis of the material and fabrication of the scaffold should be suitable for commercialization. The ease as well as reproducibility should be considered to select a processing route to fabricate porous scaffolds. The scaffolds should have good enough compressive strength, depending on the intended site of application.

A scaffold should provide an open porous network structure, allowing easier vascularization, which is important for the maintenance of penetrating cells from surrounding tissues and the development of new bone *in vivo*. The higher the macroporosity, the easier the vascularization of implant. The failure to develop an adequate vascular network means that only peripheral cells may survive or differentiate, supported by diffusion. Chang et al.<sup>56</sup> proposed that the degree of interconnectivity rather than the actual pore size has a greater influence on osteoconduction. Interconnectivity is a physical characteristic that aids in the delivery of nutrients and removal of metabolic waste products. Some studies have shown that bone normally forms in the outer 300  $\mu\text{m}$  periphery of scaffolds and that this may be explained by the lack of nutrient delivery and waste removal.<sup>57</sup> When the pore size is too small, pore occlusion can occur by cells, preventing further cell penetration and bone formation.<sup>58</sup> Pore size distributions for an ideal scaffold in bone tissue engineering applications are summarized in Table 4.1. It is pertinent to note that much higher rate of mass transfer exists at the periphery of a scaffold and that these higher rate promote mineralization, further limiting the mass transfer of nutrients to the core of a scaffold.<sup>59</sup> It is essential that a scaffold possess a high degree of interconnectivity in conjunction with a suitable pore size to minimize pore occlusion.

#### 4.5 AN EXCULPATION OF POROUS SCAFFOLDS

The concept behind nearly inert, microporous bioceramics is the ingrowths of tissue into pores on the surface or throughout the implant. The porosity is a critical factor for growth and integration of a tissue into the bioceramic implant. In particular, the open porosity, which is connected to the outside surface, is critical to the integration of tissue into the ceramic, especially if the bioceramic is inert. The increased interfacial area between the implant and the tissues results in an increased inertial resistance to movement of the device in the tissue. The interface is established by the living tissue in the pores. This method of attachment is often termed *biological fixation*. The limitation associated with porous implants is that for tissue to remain viable and healthy, it is necessary for the pores to be greater than 100–150  $\mu\text{m}$  in diameter. The large interfacial area required for the porosity is because of the need to provide blood supply to the ingrown connective tissue. Vascular tissue does not appear in pores, which measure less than 100  $\mu\text{m}$ . If micromovement occurs at the interface of a porous implant, tissue is damaged, the blood supply may be cut off, tissue dies, inflammation ensues, and the interfacial stability can be destroyed.

The potential advantage offered by a porous ceramic is the inertness combined with the mechanical stability of the highly convoluted interface when the bone grows into the pores of a ceramic. The mechanical requirements of prostheses, however, severely restrict the use of low strength porous ceramics to low-load or nonload-bearing applications. Studies show that when load bearing is not a primary requirement, nearly inert porous ceramics can provide a functional implant. Apart from biological aspects, the mechanical requirement should also be fulfilled by the engineered implant.

The necessity for porosity in bone regeneration has been shown by Kuboki et al.<sup>60,61</sup> using *in vivo* experiments in a rat model. Solid and porous particles of HA for bone morphogenic protein 2 (BMP-2) delivery were investigated simultaneously. Whereas no new bone formation was found on the solid particles, in the porous scaffolds, direct osteogenesis occurred. Further support comes from studies with porous-coated metallic implants compared with noncoated material. The treatment of titanium alloy implant surfaces with sintered titanium beads created a porous coating that enhanced the shear strength of the implants recovered from sheep tibia, but further coating with HA beads did not result in significant improvement. Titanium fiber-metal porous coatings (45% porosity and 350  $\mu\text{m}$  average pore size) maximized bone ingrowth and increased the potential for stress-related bone resorption of femoral stems in a canine total hip arthroplasty model.<sup>62</sup> A similar result was observed for plasma spray-coated titanium implants with 56–60% porosity, although bone ingrowth was maximized for an open-pore titanium fiber mesh (60% porosity and 170  $\mu\text{m}$  average pore size) coated with polyvinyl alcohol hydrogel.<sup>63</sup> D’Lima et al.<sup>64</sup> showed that surface roughness was more important for osseointegration of titanium implants in rabbit femurs because an acid-etched coating (highest surface roughness) showed a higher overall osseointegration compared with grit-blasted fiber mesh (average pore size, 400  $\mu\text{m}$ ) coatings. The coating of titanium alloy implants with a 50  $\mu\text{m}$  layer of porous HA did not increase the percentage of osseointegrated surface in the mandibles of dogs, although bone extended into the micropores of HA, resulting in an osseous micointerlocking.<sup>65</sup> However, there was more bone opposing the coated implants in the maxillae, suggesting a beneficial effect for areas of poorer bone quality. Although macroporosity (pore size  $\sim$ 450  $\mu\text{m}$ ) has a strong impact on osteogenic outcomes, microporosity (pore size  $\sim$ 10  $\mu\text{m}$ ) and pore wall roughness play important roles as well. The HA ceramic rods with average pore size of 200  $\mu\text{m}$  and smooth and dense pore walls failed to induce ectopic bone formation in dogs in contrast to rods made from the same material with average pore size of 400  $\mu\text{m}$  but with rough and porous pore walls.

Microporosity results in larger surface area, which is believed to contribute to higher bone-inducing protein adsorption as well as to ion exchange and bone-like apatite formation by dissolution and reprecipitation.<sup>66</sup> The surface roughness enhances attachment, proliferation, and differentiation of anchorage-dependent bone-forming cells. The solid free form fabrication (SFF) technique allowed the fabrication of poly(desamino tyrosyl-tyrosine ethyl ester carbonate) (a tyrosine-derived pseudopolyamino acid) scaffolds with axial and radial channels and 500  $\mu\text{m}$  pores separated by 500  $\mu\text{m}$  solid walls or 80% porous walls.<sup>66</sup> Scaffolds from the same material with random pore distributions were used as controls in the *in vivo* experiments. Although there was no statistical difference in the bone formed in cranial defects in rabbits, bone ingrowth followed the architecture of the scaffolds. A continuous ingrowth from the outer periphery was observed in the scaffolds with random pore size, but scaffolds with same sized pores and solid walls promoted discontinuous ingrowth with bone islands throughout the entire scaffold. The scaffolds with same-sized pores and porous walls resulted in both types of bone ingrowths. It was hypothesized that discontinuous bone ingrowth may result in faster healing because bone forms not only from the margins but also throughout the entire

space of the defect.<sup>67</sup> These studies demonstrate the enhanced osteogenesis of porous versus solid implants, both at the macroscopic as well as the microscopic level.

#### 4.6 OVERVIEW OF VARIOUS PROCESSING TECHNIQUES OF POROUS SCAFFOLD

A tissue-engineered scaffold must provide a germane environment for *in vitro* cell culturing in a bioreactor as well as providing a suitable environment after being implanted *in vivo*. These two environments differ in terms of nutrient concentration gradients, pressure gradients, and fluid velocities. *In vivo*, whereas diffusion is the primary mechanism for transporting nutrients, fluid flow is the principal mechanism for transport of nutrients and provision of mechanical stimuli *in vitro*.

For a scaffold to be considered successful, it is essential that it provides a nutrient-rich environment within the scaffold core for cells to lay down new matrix and minimize cell necrosis. The scaffolds with defined interconnected channels aid in the processes of cell nutrient delivery, waste removal, and vascular invasion.

Many of the conventional techniques yield scaffolds with random porous architectures, which do not necessarily produce a suitable homogeneous environment for bone formation (Fig. 4.7). Nonuniform microenvironments produce regions with

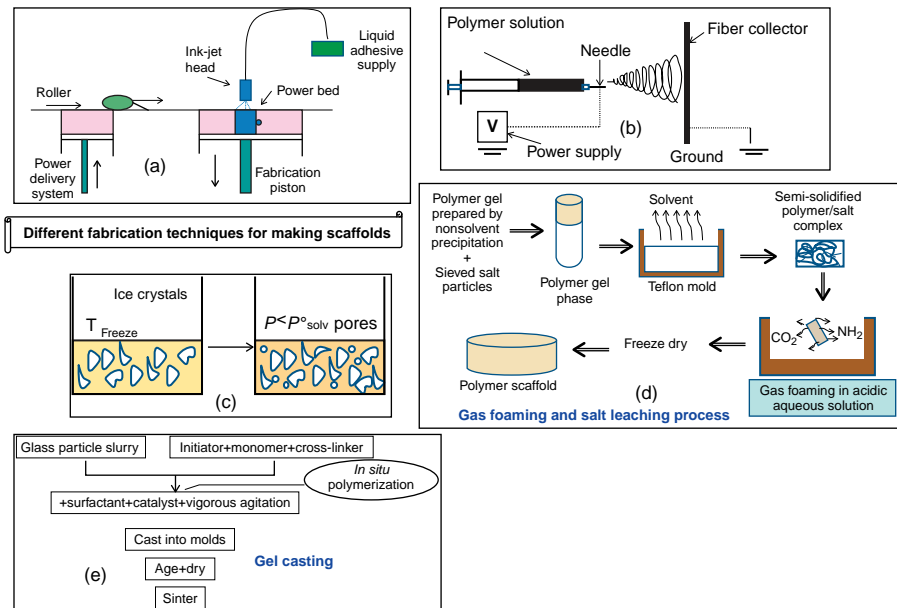


**FIGURE 4.7** Schematic illustration of different fabrication process for making porous scaffolds for tissue engineering: rapid prototype three-dimensional printing (a), electrospinning (b), Freeze casting (c), gas foaming and salt leaching (d), and gel-casting method (e).

insufficient nutrient concentrations, which can inhibit cellular activity and prevent the formation of new tissue. In the following discussion, some of the widely used processing routes are briefly described to illustrate how porous scaffolds can be fabricated.

*Rapid prototyping* is the most common name given to a host of related technologies that are used to fabricate physical objects directly from computer-aided design (CAD) data sources. These methods are unique in that they add and bond materials in layers to form objects. Such systems are also known by the names *additive manufacturing*, *additive fabrication*, *3D printing* (Fig. 4.7a), *SFF*, and *layered manufacturing*. The advantages of this process are

1. Objects can be formed with any geometric complexity or intricacy without the need for elaborate machine setup or final assembly.
2. Rapid prototyping systems reduce the construction of complex objects to a manageable, straightforward, and relatively fast process.

A number of logical steps are to be sequentially followed in the 3D printing of solids. After providing the input based on CAD design, the loose powder is transferred from the powder delivery bed to the fabrication piston bed one layer at a time in the 3D printing setup. After each layer of loose powder has been transferred, an inkjet head (similar to an inkjet printer) dispenses a polymeric or liquid binder to only select areas, binding the powder in these areas and leaving the rest loose. After a layer is done, the fabrication piston moves down the platform, the roller spreads a new layer of loose powder over the previous layer, and the process repeats. The inkjet head is controlled by a computer that accepts CAD information, allowing superior control over the structure to be built. The loose powder from the previous layer acts as support material for the next layer, enabling overhanging structures to be built. After the build, the binder is cured at slightly elevated temperature, allowing all unbound powder to be removed by gentle agitation. Depending on powder and binders, a high-temperature heat treatment process sinters the bound particles, while the binder volatilizes, leaving a three-dimensional structure. Since the invention of 3DP process,<sup>68–78</sup> this process has been largely used to fabricate solid structures with different sizes and shapes with limited efforts in making porous materials.<sup>79–81</sup>

*Electrospinning* (Fig. 4.7b) is considered the most efficient technique for micro- and nanofiber production and one of the few processes to produce polymeric fibers on a large scale. Many applications of electrospinning are related to the biomedical field. In particular, electrospun polymeric fibers were used for the production of scaffolds for vascular tissue engineering<sup>82–84</sup> or hollow organ substitutes such as the bladder, trachea, and esophagus.<sup>85–88</sup> In this method, polymer solution is injected through a needle, which is maintained at a critical voltage (to create charge imbalance) and placed in the proximity to a grounded target. At critical voltage, charge imbalance begins to overcome the surface tension of the polymer fibers, forming an electrically charged jet. Grounded target is a rotating mandrel, which collects polymeric fibers.

Although requirements for medical scaffolds are numerous and vary with every application, some of them are fulfilled by the processing technique itself.<sup>89</sup> The architecture of the fibrous scaffold produced by electrospinning displays a high surface area for initial cell attachment and porosity for improved cell infiltration and nutrition diffusion, thus providing some key features of the native extracellular matrix.

*Freeze casting* (Fig. 4.7c) is a method in which rapid freezing of a colloidal stable suspension of HA particles in a nonporous mold takes place followed by sublimation of the frozen solvent under cold temperatures in vacuum. A different technique involving gas as a porogen has been introduced to develop porous scaffolds; this commonly known as *gas foaming* (Fig. 4.7d). The process begins with the formation of solid discs of poly(lactic-co-glycolic acid) (PGA), poly(L-lactic acid) (PLLA), or poly(lactic-co-glycolic acid) (PLGA) using compression molding with a heated mold. *Gel casting* (Fig. 4.7e), an advanced process for forming ceramics, was originally developed at ORNL to make complex-shaped automotive parts such as turbines. Gel casting is a wet ceramic-forming technique that involves the polymerization of a monomer in the presence of a solvent to form a rigid, ceramic-loaded body, which can be machined directly in a complex mold.<sup>90</sup> After gel formation, gel-cast green samples can be easily demolded and are then dried in controlled conditions.<sup>91</sup> The main advantage of this new process for making high-quality, complex-shaped ceramic parts is the lower cost compared with conventional forming techniques. In addition, gel casting appears attractive for an increasing number of applications ranging from accelerator magnets to artificial bone. A gel-cast part is soft enough to be machined quickly by less costly carbon steel tools.

*Slip casting* is a technique for making multiple, essentially identical parts inexpensively. Slip-casting methods provide superior surface quality, density, and uniformity in casting high-purity ceramic raw materials over other ceramic casting techniques, such as hydraulic casting, because the cast part is at a higher concentration of ceramic raw materials with little additives. A slip is a suspension of fine powders in a liquid such as water or alcohol with small amounts of secondary materials such as dispersants, surfactants, and binders. Early slip casting techniques used a plaster block or a flask mold. The plaster mold draws water from the poured slip to compact and form the casting at the mold surface. This forms a dense cast form, removing deleterious air gaps and minimizing shrinkage in the final sintering process.

*A replication technique* has also been used to prepare highly porous material with controllable pore sizes from inorganic materials and polymer materials. This technique is a multistep procedure in which first a replica of the porous structure is made from wax, polymer, or another material that can easily be removed by melting, burning, or dissolution. This replica is then used as a negative casting mold, and the interstices are filled with the desired polymer in the liquid phase. After hardening of the liquid polymer by curing, cooling, or precipitation, the mold forming the pore network is removed. A summary of conventional scaffold processing techniques as well as their advantages and disadvantages are summarized in Table 4.2.<sup>92,93</sup>

**TABLE 4.2 Conventional Scaffold Processing Techniques for Tissue Engineering**<sup>93,94</sup>

Process	Advantages	Disadvantages
Solvent casting and particulate leaching	Large range of pore sizes	Limited membrane thickness (3 mm)
	Independent control of porosity and pore size	Limited interconnectivity
	Crystallinity can be tailored	Residual porogens
	Highly porous structures	Poor control over internal architecture
Fiber bonding	High porosity	Limited range of polymers Residual solvents Lack of mechanical strength
Phase separation	Highly porous structures	Poor control over internal architecture
	Permits incorporation of bioactive agents	Limited range of pore sizes
Melt molding	Independent control of porosity and pore size	High temperature required for nonamorphous polymer
	Macro shape control	Residual porogens
Membrane lamination	Macro shape control	Lack of mechanical strength
	Independent control of porosity and pore size	Limited interconnectivity
Polymer–ceramic fiber composite foam	Independent control of porosity and pore size	Problems with residual solvent
	Superior compressive strength	Residual porogens
High-pressure processing	No organic solvents	Nonporous external surface Closed-pore structure
		Limited to small pore sizes
Freeze-drying	Highly porous structures	
	High pore interconnectivity	
Hydrocarbon templating	No thickness limitation	Residual solvents
	Independent control of porosity and pore size	Residual porogens

## 4.7 OVERVIEW OF PHYSICOMECHANICAL PROPERTIES EVALUATION OF POROUS SCAFFOLD

Although increased porosity and pore size facilitate bone ingrowth, the result is a reduction in mechanical properties because this compromises the structural integrity of the scaffold. The increased porosity resulted in a higher median pore size (0.2–8.7  $\mu\text{m}$ ) and lower percentage of nanopores (<100 nm).<sup>94</sup> At the same time, lower compressive strength (37,000–430 kPa) and Weibull modulus (2.0–4.2) were reported.

Porous foams were fabricated by sintering poly(lactide-*co*-glycolide) microspheres. An increase in the microsphere diameter from 212–250  $\mu\text{m}$  to 600–710  $\mu\text{m}$  resulted in larger median pore size (72–164  $\mu\text{m}$  for 2 h of heating and 101–210  $\mu\text{m}$  for 4 h of heating) and a wider pore distribution (38–110  $\mu\text{m}$  in size, respectively) but had no effect



on total porosity. The compressive modulus was decreased from 297 to 232 MPa.<sup>95</sup> Similarly, higher porosity (80% vs. 58%) decreased mechanical properties of porous poly(L-lactide-co-D,L-lactide) scaffolds as compressive strength decreased from 11.0 to 2.7 MPa and modulus from 168.3 to 43.5 MPa.<sup>96</sup> The porosity of these scaffolds was ~80% because lower porosity resulted in less interconnected pores<sup>97</sup> and higher porosity results in low mechanical properties.<sup>98</sup> Higher porosity (48% vs. 44%) of cancellous structured titanium surface coating of dental implants resulted in lower tensile strength (16.1 vs. 31.7 MPa).<sup>99</sup> In general, the compromise in mechanical properties of the scaffold with increasing porosity sets an upper limit in terms of porosity and the pore size that can be tolerated.

Koc et al.<sup>100</sup> fabricated and characterized porous tricalcium ceramics using a modified slip-casting technique. The slip was prepared by suspending custom-made tricalcium phosphate (TCP) powder and poly(methyl methacrylate) (PMMA) beads in an aqueous medium stabilized with an acrylic deflocculant. Porous TCP ceramics were obtained by sintering the polymer-free preforms for 2 h at 1000°C. The ceramic was prepared from a casting slip, which contained 70% polymer beads in the size range of 210–250  $\mu\text{m}$ . The average size of large pores in the sintered ceramic was around 190  $\mu\text{m}$ . Koc et al.<sup>100</sup> suggested that higher proportions of polymer beads in slip solids led to the development of highly porous ceramics with thinner walls. As the amount of polymer beads was raised, the size of interconnections increased proportionately. It was concluded that porosity network of this nature would allow free circulation of body fluids.

Li et al.<sup>101</sup> studied novel method to manufacture porous hydroxyapatite by dual phase mixing. Their technique was based on mixing the immiscible phases of HA slurry and PMMA resin. Naphthalene particles were embedded to get >50% porosity. The majority of pores could be located within the range of 200–300  $\mu\text{m}$  for HA with 50% porosity. The average compressive strength was reported as 8.9 MPa for 50% porous HA and was only 4.8 MPa for HA with 60% porosity. They also concluded that by controlling the process parameters such as the viscosity of HA slurry, the HA–PMMA ratio or the mixing time and speed, it is possible to adjust porosity, pore size, and interconnectivity.

Uniform porous hydroxyapatite scaffolds were also prepared by using another solid phase, which was completely burnt out at the time of sintering. Polystyrene microspheres were used by Tang et al.,<sup>102</sup> and they developed HA material of varying diameter and porosity (diameter,  $436 \pm 25$  nm,  $892 \pm 20$  nm, and  $1890 \pm 20$  nm; porosity, 46.5%, 41.3%, and 34.7%, respectively). On the other hand, Itatani et al.<sup>103</sup> used  $\text{H}_2\text{O}_2$  as a foaming agent and found that by changing the concentration of  $\text{H}_2\text{O}_2$  solution from 0 to 20 mass%, HA compact exhibited pore sizes with maximum porosity (71.7%) at around 0.7  $\mu\text{m}$ , 5–100  $\mu\text{m}$ , and 100–200  $\mu\text{m}$ . In a different work, Thijs et al.<sup>104</sup> studied a novel technique to produce macroporous ceramics using seeds and peas as sacrificial core materials. The first step in this technique was to coat the seeds and peas with wetting ceramic slurry that undergoes gelation. The coated seeds and peas were consolidated by packing them in a container and infiltrating with ceramic slurry, which underwent gelation. The compacts thus obtained were subjected to the conventional steps of drying, binder burnout, and sintering. The

resulting bodies had greater than 90% porosity with pore size determined by the size of the seeds or peas.

The polymer replication or sponge technique is another commonly used process to develop porous scaffolds for artificial bone applications. Ramay et al.<sup>105</sup> developed the porous HA scaffold having apparent densities of 0.04–0.78 g/cm<sup>3</sup> and compressive strength of 0.55–5 MPa (Figs. 4.8a and 4.9). Similarly, Sopyan et al.<sup>106</sup> adopted a similar processing route and reported enhanced properties. They reported the compressive strength ranging from 1.3 to 10.5 MPa for the increased apparent density from 1.27 to 2.01 g/cm<sup>3</sup>. It was concluded that the homogeneity of slurry and the effect of heating rate on porosity and density of porous bodies in turn influenced the compressive strength. More homogeneous slurries and a faster heating rate gave porous bodies with the increased compressive strength caused by a higher apparent density and crystallinity.

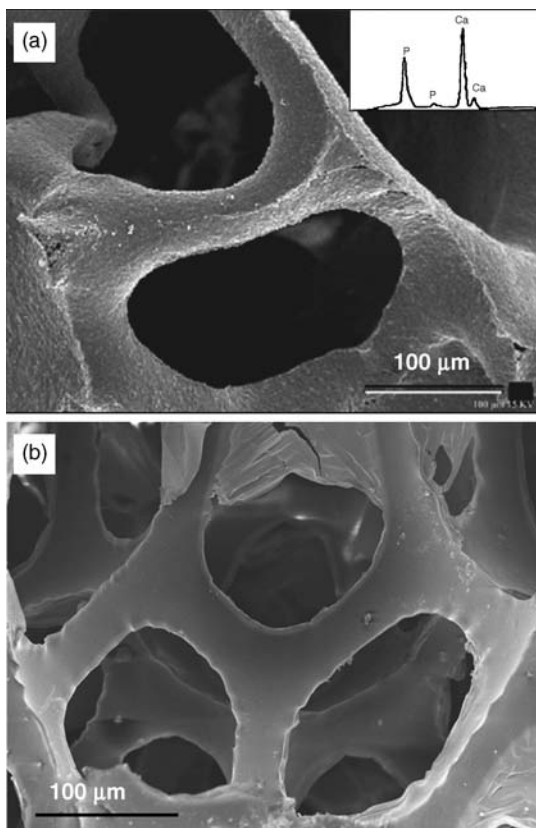


**FIGURE 4.8** Scanning electron microscope (SEM) micrographs of an HA scaffold showing the sintered structure of the pore walls and pores. (a) At struts with EDS spectrum as an inset showing the amount of Ca and P present in the sintered scaffold. Printed with permission from Ref. 129. (b) SEM micrograph of an HA scaffold sol-gel derived HA powder and polymer slurry. Printed with permission from Ref. 129.

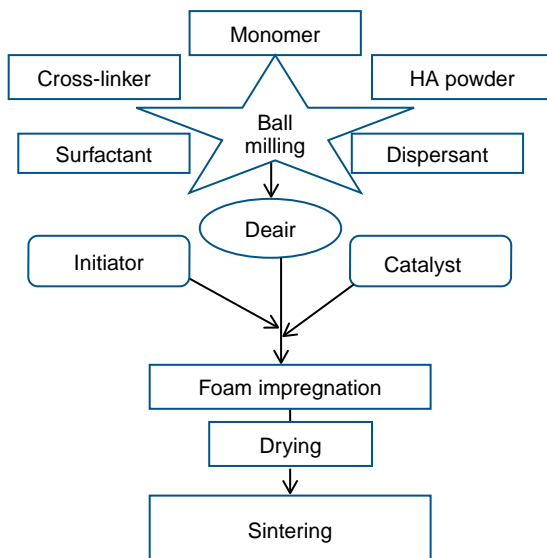


**FIGURE 4.9** A flow chart of process steps for scaffold fabrication using combined gel-casting and polymer sponge methods. Idea adapted from Ref. 105.

The present authors<sup>107</sup> also developed the macroporous HA scaffolds using polymer sponge replication method with interconnected oval-shaped pores of 100–300  $\mu\text{m}$  with a pore wall thickness of  $\sim 50 \mu\text{m}$  (Fig. 4.8b). The obtained compressive strength of 60 wt% HA loaded scaffold was calculated 1.3 MPa. The biological response of the scaffold was investigated using human osteoblast-like SaOS<sub>2</sub> cells. Their results showed that SaOS<sub>2</sub> cells were able to adhere, proliferate, and migrate into pores of scaffold. Furthermore, the cell viability was found to increase on porous scaffold compared with dense HA. They also investigated the expression of alkaline phosphatase and concluded that the differentiation marker for SaOS<sub>2</sub> cells was enhanced for porous HA scaffold compared with nonporous HA disc with respect to the number of days of culture (Fig. 4.10).

Successful fabrication of porous bioceramic using polyurethane (PU) sponge was reported by Soon-Ho Kwon et al.<sup>108</sup> Porosity was controlled by the number of coatings on the sponge struts. Single coating results in a porosity of  $\sim 90\%$ , where as five-layered coating gave rise to 65% porosity. In both cases, the pores were completely interconnected. The compressive strength was strongly dependent on the porosity and weakly dependent on the type of ceramics: HA, TCP, or HA–TCP composite. At 65% porosity level, the strength was  $\sim 3$  MPa. The TCP exhibited the highest dissolution rate in a Ringer's solution, while HA had the lowest rate. The biphasic HA–TCP composite showed an intermediate dissolution rate. The biodegradation of calcium phosphate ceramics could be controlled by simply adjusting the amount of HA or TCP in the ceramic.

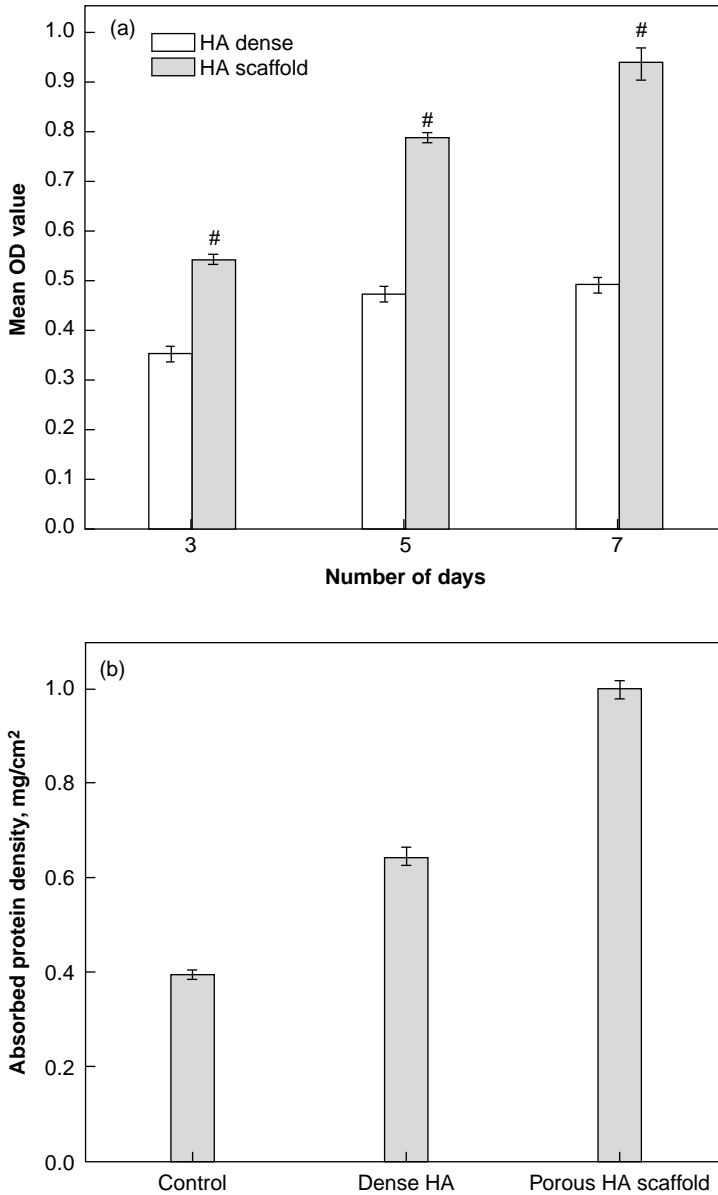


**FIGURE 4.10** (a) ALP assay results showing the SaOS<sub>2</sub> cell response on dense HA and microporous HA scaffold after 3, 5, and 7 days of culture. *Asterisks* represent significant difference at  $P < 0.05$  with respect to compositions, and error bars correspond to  $\pm 1.00$  SE for number of days of culture. (b) Comparison of BSA protein absorption behavior of scaffold with dense HA and a negative control disc after incubation for 4 h. Idea adapted from Ref. 107.

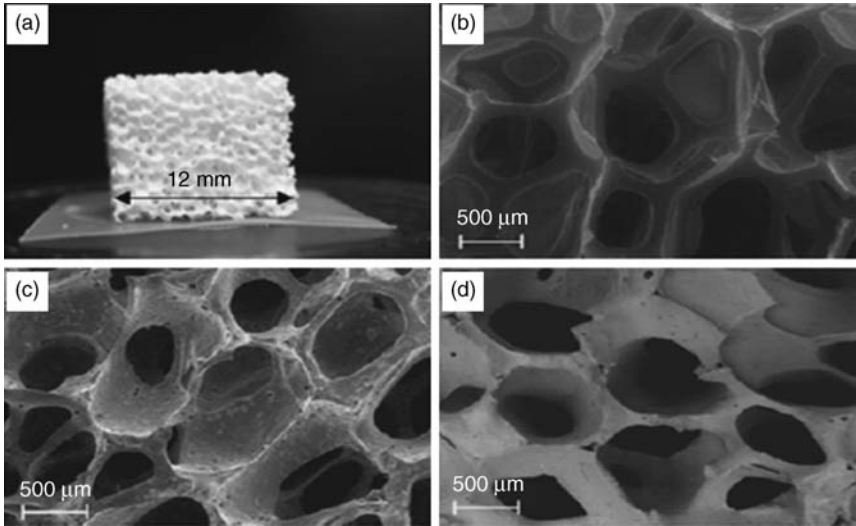


**FIGURE 4.11** A macrograph of a porous scaffold (a), SEM image of the macrostructure of the sponge (b) and of the scaffolds sintered at 1300°C with the in-laboratory synthesized powder (c), and the commercial powder (d). The porosity is open and highly interconnected in both of the samples. Idea adapted from Ref. 109.

Gervaso et al.<sup>109</sup> produced porous scaffolds with a polymer sponge templating method using reactive submicrometer powders synthesized by a hydroxide precipitation sol–gel route. The templating method ensured a highly interconnected macrochanneled porous structure with a more than 500 μm mean pore size and 90% porosity (Fig. 4.11). The high reactivity of the powder led to an efficient sintering mechanism with a high and crack-free linear shrinkage ( $19 \pm 2\%$ ) and a significant BET-specific surface area reduction (from 12 to 0.33 m<sup>2</sup>/g). The powder does not dissociate into secondary phases during sintering. Despite the extreme porosity, the scaffolds had high mechanical performance (compressive strength  $\sim 0.51$  MPa; Weibull modulus  $\sim 4.15$ ) compared with similarly prepared scaffolds from high-quality commercial HA powder (Fig. 4.12).

The slurry infiltration process for making porous ceramics was studied by Schwartzwalder and Somers.<sup>110</sup> In this process, PU foam was infiltrated with ceramic slurry, and the body was compressed by passing it through a set of rollers to remove the excess slurry. In this manner, the slurry remained coated on the PU struts, and open pore channels were left in between. The coated PU foam was then dried followed by burnout of the PU and sintering at a higher temperature. The foams produced were reticulated foams with porosity within the range of 75–90%.

Zhu et al.<sup>111</sup> investigated the influence of the compressive strain during roll pressing and the number of passes on the foam microstructure. It was seen that the quality of slurry coating on to PU struts was strongly dependent on the magnitude of compressive strain rather than the number of passes. Higher compressive strain resulted in thinner slurry coating on the struts and a lower bulk density. The coating

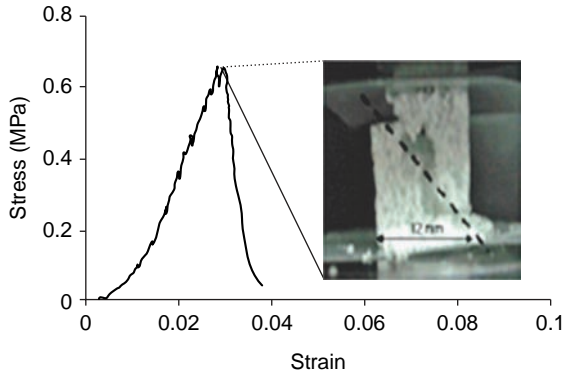


**FIGURE 4.12** Stress–strain curve of an SL scaffold subject to compression test. In the inset is a picture of the failure of the sample that occurs at the peak of the stress. Idea adapted from Ref. 109.

of slurry onto PU struts was also affected by slurry viscosity. Highly fluid slurries were not very effective in coating the PU foam struts, resulting in accumulation of slurry at the bottom of PU foam. On the other hand, Pu et al.<sup>112</sup> pointed out that the conventional roll-pressing procedure results in accumulation of slurries at the joint of the polymeric struts. Lin et al.<sup>113</sup> focused on the preparation of macroporous calcium silicate ceramics using PEG as a pore former. The sintered compacts with porosity in the range of 40–75% have been obtained by varying the amount and size of ceramic and PEG particles and the sintering temperature. The molecular weight of PEG plays an important role in the morphology, structure, and the pore size of the microporous calcium silicate. Also, PEG plays a main role in larger pore formation when enough mass of PEG with lower molecular weight is added.

A novel combination of PU foam method and a hydrogen peroxide ( $H_2O_2$ ) foaming method was used to fabricate the macroporous HA scaffolds.<sup>114</sup> Such scaffolds have a unique macroporous structure and special struts of polymer–ceramic interpenetrating composites. Micropores were present in the resulting porous HA ceramics after infiltration with PLGA polymer. The internal surfaces of the macropores were further coated with a PLGA bioactive glass composite. It was found that the HA scaffolds fabricated by the combined method show high porosities of 61–65% and proper macropore sizes of 200–600  $\mu\text{m}$ . The PLGA infiltration improved the compressive strengths of the scaffolds from 1.5–1.8 MPa to 4.0–5.8 MPa.

Similarly, Narbat et al.<sup>115</sup> fabricated porous HA–gelatin composite scaffolds. They reported that the prepared scaffold has an open, interconnected porous structure with the pore size of 80–400  $\mu\text{m}$ , which is suitable for osteoblast cell proliferation. The mechanical properties of the scaffolds with different weight fraction of HA (30, 40, and 50 wt%) was assessed, and it was found that the gelatin–HA with a ratio of 50 wt% HA has the compressive modulus of  $\sim 10$  GPa, the ultimate compressive strength of  $\sim 32$  MPa. The porosity and the apparent density of 50 wt% HA scaffold were calculated, and it was found that the addition of HA could reduce the water absorption and the porosity.

The demonstration of potato starch as both a consolidator or binder and a pore former in forming porous ceramics was reported by Lyckfeldt and Ferreira.<sup>116</sup> In this process, 16–60% starch was added as dry powder weight basis to ceramic slips and homogenized for 2 h. The homogenized slip was consolidated in a mold at 80°C followed by drying, binder burnout, and finally sintering. The pore sizes in the range 10–80  $\mu\text{m}$  and porosity between 23% and 70% were obtained by varying ceramic loading and the nature and amount of starch. Importantly, increasing the amount of a specific type of starch resulted in a large pore size because of a greater degree of contact among the starch particles.

The freeze-casting route can produce porous HA scaffolds with porosities in the range of 40–60%.<sup>117</sup> By adopting this route, the pores were open and unidirectional and exhibited a lamellar morphology. Such a porous scaffold has a compressive strength of 145 MPa. Potoczek<sup>118</sup> studied the gel casting of HA foams using agarose as gelling agent. The viscosity of the slurries could be adjusted by agarose concentration and HA solid loading. These parameters were essential in tailoring the porosity as well as the cell and window sizes of the resulted HA foams. Depending on HA solid loading (24–29 vol%) and agarose concentration (1.1–1.5 wt% with regard to water) in the starting slurry, the mean cell size ranged from 130 to 380  $\mu\text{m}$ , and the mean window size varied from 37 to 104  $\mu\text{m}$ . Depending on the porosity range (73–92%) and the mean cell and window size, the compressive strength of HA foams was found to be in the range of 0.8–5.9 MPa.

Chloroform as a binder was used to fabricate porous scaffold in a 3DP route by Giordano et al.<sup>119</sup> They studied the mechanical properties of 3DP processed PLLA parts. Test bars were fabricated from low- and high-molecular-weight PLLA powders. The binder printed per unit length of the powder was varied to analyze the effects of printing conditions on mechanical and physical properties of the PLLA bars. The maximum measured tensile strength for the low-molecular-weight PLLA (53,000 g/molecule) was  $17.4 \pm 0.7$  MPa and for high-molecular-weight PLLA (312,000 g/molecule) was  $15.9 \pm 1.5$  MPa. Kim et al.<sup>120</sup> evaluated the survival and function of hepatocytes on a scaffold with an intrinsic network of interconnected channels under continuous flow conditions. The scaffolds were designed and fabricated using the technique of 3DP on copolymers of polylactide–coglycolide (PLGA 85:15). 3DP was also used to selectively direct a solvent onto PLGA powder particles packed with sodium chloride particles (45–150  $\mu\text{m}$ ). The polymer scaffolds were fabricated in the shape of a cylinder of 8 mm in diameter and 7 mm in height. They contained 12 interconnected longitudinal channels (800  $\mu\text{m}$  in diameter) running through the length of the scaffold and 24 interconnected radial channels (800  $\mu\text{m}$  diameter) at various lengths of the devices. The salt crystals were leached out to yield porous devices of 60% porosity with micropores of 45–150  $\mu\text{m}$  in diameter. The fabrication of scaffolds for tissue engineering requires choosing a conformation method that yields pieces with interconnected porosity and pores in the 20–400  $\mu\text{m}$  range.<sup>121</sup>

Table 4.3 lists some selected typical physical and mechanical properties of scaffolds obtained by various processing routes. A similar material was processed under different processing techniques, which result in varying physical properties.

**TABLE 4.3 An Overview of Various Processing Techniques Used to Develop Porous Scaffolds with Varying Pore Sizes and Properties**

Technique	Material	Open Porosity	Pore Size or Dimension ( $\mu\text{m}$ )	Compressive Strength (MPa)	Reference
Freeze casting	HA	47–52	5–30	12–18	[124]
	HA	50–60	80–110	7.5–20	[125]
	HA	40–65	20	40–145	[122,123]
Polymer sponge	HA–polycaprolactone	87	150–200	–	[126]
	HA, PHBHHx, dioxane	88–92	–	–	[127]
	HA	86	420–560	0.21	[128]
	Glass-reinforced HA	85–97.5	420–560	0.01–0.18	[129]
	HA	70–77	200–400	0.55–5.0	[130]
	45S2 bioglass	89–92	510–720	0.27–0.42	[131]
	HA	–	100–200	–	[132]
	HA	–	100–400	–	[133]
	HA–TCP	36	100–150	–	[134]
	Ca <sub>2</sub> MgSi <sub>2</sub> O <sub>7</sub>	63–90	300–500	0.53–1.13	[135]
Gel casting	HA, polyvinyl alcohol, acetone	85	–	–	[136]
	HA	76–80	20–1000	4.4–7.4	[137]
	HA	72–90	17–122	1.6–5.8	[138]
Slip casting	HA–PMMA	–	200–400	5.0	[139]
	13–93 glass	40–45	100–300	21–23	[140]
Gas foaming	HA	85	200–500	1.09–1.76	[141]
	PLGA	85–96	193–439	0.16–0.29	[142]
Salt leaching	<i>n</i> -HA/PU	80	100–800	0.27	[143]
	TCP cement calcium metaphosphate	–	200	–	[144]

HA, hydroxyapatite; PLGA, poly(lactic-co-glycolic acid); PMMA, polymethylmethacrylate; PU, polyurethane; TCP, tricalcium phosphate.



It can be summarized from Table 4.3 that the variation in pore size and open porosity directly affects the mechanical behavior of the prepared scaffold. The freeze-casting method provides the highest compressive strength of around 40–145 MPa. The lower strength (<1 MPa) of porous constructs was obtained in the polymer sponge method and gas-foaming process. Recent investigations have shown that porous HA scaffolds, with a lamellar-type microstructure and unidirectional pores, can be obtained by freeze casting of aqueous suspensions.<sup>122,123</sup>

#### 4.8 OVERVIEW OF BIOCOMPATIBILITY PROPERTIES: EVALUATION OF POROUS SCAFFOLDS

Karageorgiou and Kaplan<sup>145</sup> investigated the influence of porosity on osteogenesis in three-dimensional biomaterial scaffolds. It has been seen that the porosity and pore size of biomaterial scaffolds play critical roles in bone formation *in vitro* and *in vivo*. The minimum requirement for pore size is considered to be  $\sim 100\ \mu\text{m}$  because of cell size and migration requirements. However, pore sizes of  $\sim 300\ \mu\text{m}$  are recommended because of enhanced new bone formation and the formation of capillaries. The effect of these morphological features on osteogenesis *in vitro* and *in vivo*, as well as relationships to mechanical properties of the scaffolds, was addressed. *In vitro*, lower porosity stimulates osteogenesis by suppressing cell proliferation and forcing cell aggregation. In disparity, higher porosity and pore size result in greater bone ingrowth *in vivo*.

The kinetics of bone-like apatite formation on sintered hydroxyapatite in a simulated body fluid was studied by Kim et al.<sup>146</sup> The surfaces of two HAs, which have been sintered at different temperatures of 800°C and 1200°C, were investigated as a function of soaking time in simulated body fluid (SBF) using transmission electron microscopy (TEM) attached with energy-dispersive spectrometry (EDX) and laser electrophoresis spectroscopy.

The synthesis of biomimetic Ca-hydroxyapatite powders at 37°C in synthetic body fluids was reported by Tas.<sup>147</sup> Initially, HA was prepared as a nanosized ( $\sim 50\ \text{nm}$ ), homogeneous, and high-purity ceramic powder from calcium nitrate tetrahydrate and diammonium hydrogen phosphate salts dissolved in modified SBF solutions at 37°C and a pH of 7.4 using a novel chemical precipitation technique. The synthesized precursors were found to reach a phase purity of 99% easily after 6 h of calcination in air atmosphere at 900°C after oven-drying at 80°C.

Biocompatibility and osteogenicity of degradable Ca-deficient hydroxyapatite (CDHA) scaffolds were investigated by Guo and coworkers.<sup>148</sup> They made scaffold from calcium phosphate cement for bone tissue engineering with a particle-leaching method. They demonstrated that the CDHA scaffolds with porosity of 81% showed open macropores with pore sizes of 400–500  $\mu\text{m}$ . Thirty-six percent of these CDHA scaffolds were degraded after 12 weeks in Tris–HCl solution. The results revealed that the CDHA scaffolds were biocompatible and had no negative effects on the mesenchymal stem cells (MSCs) *in vitro*. The CDHA scaffold, after 8 week implantation in rabbit model shows good *in vivo* biocompatibility and extensive osteoconductivity.

Park et al.<sup>149</sup> reported the fabrication of patterned PLLA substrates with the spatial organization of cells obtained using the 3DP route. They demonstrated an integration of polymer processing and selective polymer surface modification using methods suitable for construction of three-dimensional polymer scaffolds, which may aid such cell organization. They concluded that their approach may be generally useful for creating regionally selective, microarchitected scaffolds fabricated from biodegradable polymers for spatial organization of diverse cell types.

Peng et al.<sup>150</sup> developed a novel scaffold with large dimension of 3–4 cm in length and 1–1.5 cm in diameter. They designed and fabricated the scaffold for bone tissue engineering *in vivo*. Porous HA in the form of a tube coated with a thin layer of poly(L-lactic acid) (PLA) held the HA spherules together and provided the initial strength of scaffolds. Studies on engineering of large bone tissue were underway by use of the hybrid scaffold implanted at different nonrepairing sites such as muscle, peritoneum, and bone *in vivo*. The novel scaffolds were implanted in different sites of dogs (Fig. 4.13). To compare the influence of the distribution of biological substance on the osteogenesis, the HA spherules were mixed homogeneously with comminuted bone granules before filling in the porous HA tube. The primary tissue section showed a promising new bone growth induced by the homogeneous addition of comminuted bone granules.

Becker et al.<sup>151</sup> evaluated the ability of CAD synthetic hydroxyapatite and tricalcium phosphate blocks to serve as scaffolds for intramuscular bone induction

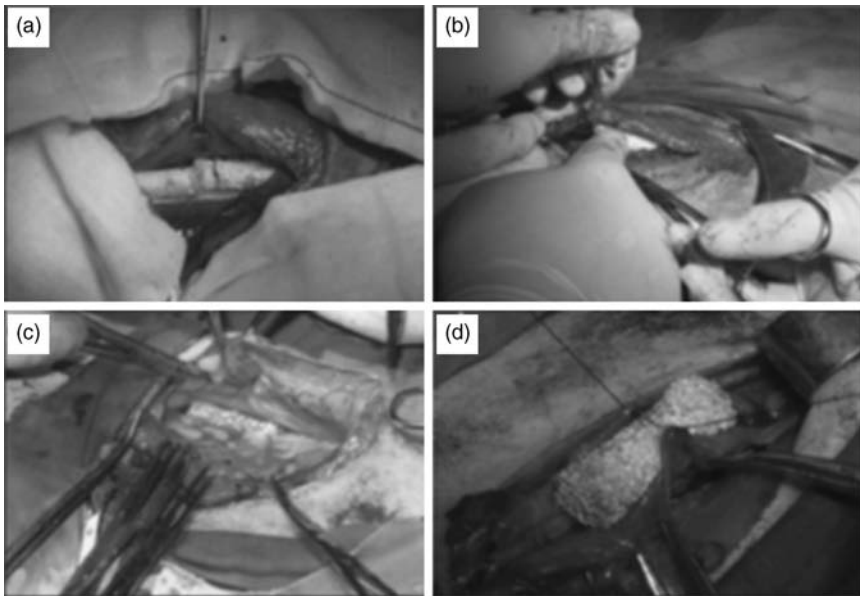


**FIGURE 4.13** Digital photos showing the implantation of the porous scaffold at different sites of natural bone: beside the femur (a), in the muscle (b), in the abdominal cavity (c), and in the peritoneum pocket (d). Printed with permission from Ref. 129.

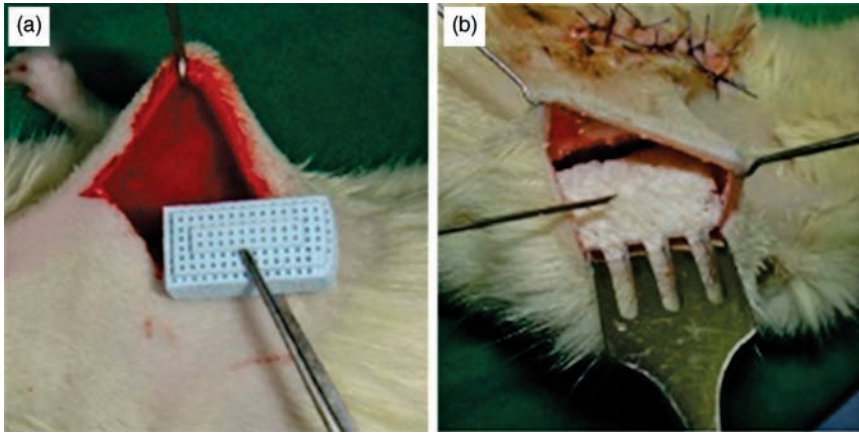


**FIGURE 4.14** Digital photographs illustrating (a) insertion of a hydroxyapatite block into the pouch. (b) A bovine HA block was placed into the pouch on the right side. Printed with permission from Ref. 130.

in a rat model (Fig. 4.14). Individually, they kept the designed 3D-printed rounded and porous HA and TCP blocks in pouches in the musculus latissimus dorsi in 12 Lewis rats bilaterally. For 8 weeks, the bone generation was monitored by computed tomography and fluorescence labeling. For all scaffolds, toluidine staining revealed vital bone directly on the scaffold materials but also in the gaps between the walls of interconnected pores. They concluded that the specially shaped HA and TCP blocks tested against the bovine HA blocks could exhibit good biocompatibility and osteoinductivity *in vivo*.

The present authors also developed porous HA scaffolds using the polymer blend method.<sup>152</sup> In this method, PMMA was used as porogenous template to obtain micro- and mesoporosity. The pore size in the sintered ceramics was in the range of 1–50  $\mu\text{m}$ . The cell adhesion test with human osteoblast cells (SaOS<sub>2</sub>) confirmed good cytocompatibility of porous composite. Fluorescent staining of osteoblast revealed a well-developed cytoskeleton with strong stress fibers (Fig. 4.15). The ALP activity of osteoblast-like cells grown on the porous scaffolds for various culture times was significantly higher than that of dense HA. The results suggested that the porous HA–PMMA hybrid composite can be used as substrate, which should facilitate better cell differentiation than sintered HA. It is consistent with the previous reports that the polymer–HA scaffolds are superior to the pure polymer scaffolds for osseous tissue engineering<sup>153</sup> because the presence of HA hydroxyl groups could promote calcium and phosphate precipitation and improve interactions with osteoblasts.<sup>154</sup> It was concluded that such a processing approach offers a better possibility to produce porous HA scaffolds with micro- and mesopores, which can stimulate significant cell adhesion and osteoblast differentiation.

Kwon et al.<sup>155</sup> successfully fabricated porous bioceramics with varying porosity, using the PU sponge technique. When a porous solid was produced by a single coating, the porosity was  $\sim 90\%$ , and the pores were completely interconnected.

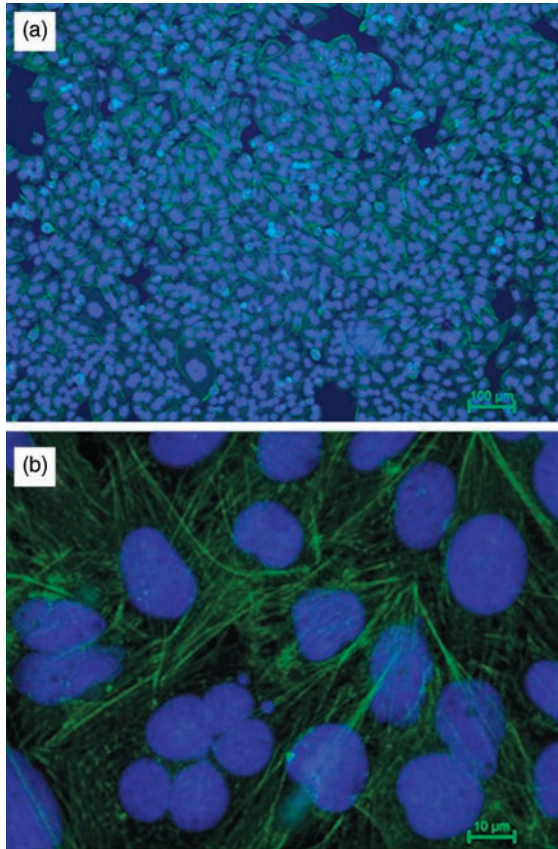


**FIGURE 4.15** Fluorescent imaging of osteoblast cells revealing a well-developed cytoskeleton with strong actin stress fibers oriented in the adhered cells in their longitudinal direction.

When the sintered ceramic was coated five times after the porous network had been made, the porosity decreased to 65%. The compressive strength was strongly dependent on the porosity and weakly dependent on the type of ceramics (i.e., HA, TCP, or HA–TCP composite). At a 65% porosity level, the strength was  $\sim 3$  MPa. The TCP exhibited the highest dissolution rate in Ringer's solution with HA exhibiting the lowest rate. The biphasic HA–TCP composite showed an intermediate dissolution rate. The biodegradation of calcium phosphate ceramics could be controlled by simply adjusting the amount of HA or TCP in the ceramic.

#### 4.9 OUTSTANDING ISSUES

Although available literature, as summarized above, provides details on synthesis, properties and different applications of porous scaffolds, it is quite clear that porous

material with desired porous architecture for specific biomedical application is still awaiting. Regardless of the type of porous scaffold (ceramic or polymer based), all tissue engineering scaffolds should meet the following requirements:

1. Surface wettability properties to promote cell adhesion, proliferation, and differentiation.
2. Mechanical properties to withstand stress.
3. Large ratio of surface area to volume to allow tissue ingrowth.
4. Controlled rate of degradation (particularly for polymer scaffolds).

In this chapter, emphasis has also been placed on the design of polymeric scaffold materials that obtain specific, desired, and timely responses from surrounding cells and tissues. The overall challenges concerning critical scaffold design parameters include polymer assembly, surface properties, nano- or macrostructure, biocompatibility, biodegradability, and mechanical properties.

From the discussion on porous scaffolds, it should be clear that multiscale porous scaffolds would be an interesting material to be developed and investigated in the future. It is known that microporosity with pore sizes of less than 1  $\mu\text{m}$  helps in initial protein adsorption, and pore sizes of 1–20  $\mu\text{m}$  aid in cell attachment as well as oriented cellular growth at the initial stage of cell proliferation and growth. Also, macroporosity with pore sizes of 100–1000  $\mu\text{m}$  facilitates tissue or bone ingrowth *in vivo*. It would be therefore ideal to produce a porous scaffold with top surface of less than 1  $\mu\text{m}$  pore size and of bioresorbable material followed by pores of 1–20  $\mu\text{m}$  size and subsequently pores of 100  $\mu\text{m}$  or larger with a top-down approach. Although the fabrication of scaffolds with such a controlled or gradient pore size could be a major challenge in terms of processing, one can use 3D printing method to produce such gradient porosity in HA–TCP or TCP–Ti system. As mentioned earlier, the type and amount of binder as well as postprinting heat treatment would be related challenges.

The potential for improving the mechanical properties of bioceramics or polymer composite scaffolds with a fabrication approach has been demonstrated in several systems with limited success to achieve mechanical properties, particularly compression strength, or modulus in the range of values for cancellous bone. All of the processing approaches can be conveniently classified into two categories: (1) chemical precursor-based routes and (2) engineering-based approaches. Although the first category largely results in uncontrolled porosity with heterogeneous or untailed pore sizes, the second category (i.e., 3D printing or other rapid prototyping routes) produces porous scaffolds with tailored porosity. More emphasis should be placed in the future to develop porous scaffolds with properties comparable to those of cancellous bone.

Another key question that needs to be addressed in future research is whether porosity in inherently bioinert scaffold material can induce bioactivity. To illustrate this issue, one can do *in vitro* or *in vivo* experiments on porous Ti and porous HA under identical conditions with similar porous architecture.

#### 4.10 CONCLUSIONS

This chapter has provided an overview of the processing and physical and biological properties that play important roles in the design of porous ceramics. Various illustrative examples of porous scaffolds have also been discussed in detail.

In summary, the design criteria and critical issues in developing porous scaffolds for bone tissue engineering have been discussed. In addition, the suitability of porous scaffolds for both *in vitro* and *in vivo* biocompatibility properties has been rationalized. Various techniques for developing scaffolds along with their advantages and disadvantages are discussed. A high degree of interconnectivity in conjunction with a suitable pore size has been emphasized for porous scaffolds to minimize diffusion and pore occlusion. However, there is a limited understanding in terms of the long-term *in vitro* and *in vivo* biocompatibility properties of porous scaffolds. In particular, the degradation and ion-release kinetics of inorganic phases from highly porous systems. For bone regeneration, the utmost challenge for porous scaffolds is to impart the mechanical strength for replacing the bone defects as well as efficient load transmission. Despite the availability of a number of fabrication techniques, the aspects of mechanical reliability of scaffolds together with induction of vascularization and tailored degradability are yet to be addressed. At present, none of the available fabrication routes offers such a combination of properties in a designed porous scaffold. Reviewing the experimental and clinical studies, it can be concluded that an ideal scaffold for tissue-engineered bone and cartilage has not yet been developed. In general, the scaffolds require individual external shape and well-defined internal structure with interconnected porosity to host most cell types. From a biological point of view, the designed matrix should serve various functions, including (1) as an immobilization site for transplanted cells; (2) formation of a protective space to prevent unwanted tissue growth into the wound bed and allow healing with differentiated tissue; and (3) directing migration or growth of cells via surface properties of the scaffold or via release of soluble molecules such as growth factors, hormones, or cytokines. At the closure, it needs to be emphasized that future studies should concentrate more on adopting engineering-based processing approaches to fabricate porous scaffolds with tailored porosity and to develop a comprehensive understanding of relationships among processing, microstructure, biocompatibility, and clinical performance. Toward this, a battery of *in vitro* biochemical assays to evaluate porosity dependence of cell fate process as well as long-term *in vivo* biocompatibility assessment in suitable animal model together with investigation on bone regeneration using microcomputer tomography as well as TEM of bone-implant interface are to be performed. In addition, molecular biology techniques, such as flow cytometry, need to be used to quantitatively assess the cell proliferation, cell cycle and cell apoptosis or reactive oxygen stress (ROS) generation for specific cell types when grown on porous scaffolds.

#### ACKNOWLEDGMENT

The authors are thankful to Department of Science and Technology, New Delhi, India, for financial support.

## REFERENCES

1. Williams DF. On the nature of biomaterials. *Biomaterials* 2009;30:5897–5909.
2. Williams DF. On the mechanisms of biocompatibility. *Biomaterials* 2008;29:2941–2953.
3. Basu B, Katti D, Kumar A. *Advanced Biomaterials: Fundamentals, Processing and Applications*. Hoboken: Wiley; 2009.
4. Chaikof EL, Matthew H, Kohn J, Mikos AG, Prestwich GD, Yip CM. Biomaterials and scaffolds in reparative medicine. *Ann NY Acad Sci* 2002;961:96–105.
5. Levenberg S, Langer R. *Advances in Tissue Engineering: Current Topics in Developmental Biology*, vol. 61. New York: Academic Press; 2004. p 113–134.
6. Griffith LG. Emerging design principles in biomaterials and scaffolds for tissue engineering. *Ann NY Acad Sci* 2002;961:83–95.
7. Karageorgiou V, Kaplan D. Porosity of 3D biomaterial scaffolds and osteogenesis. *Biomaterials* 2005;26:5474–5491.
8. Gluck T. Department of modern surgical experiment by the positive results obtained, concerning the seam and the replacement of higher tissue defect, as well as the living and utilize absorbable tampons in surgery. *Arch Clin Surg* 1891;41:187–239.
9. Energy and environmental technology materials engineering and technology. [http://www.eng-env.com/Mat\\_Eng/Biomaterials/Biomaterials.html](http://www.eng-env.com/Mat_Eng/Biomaterials/Biomaterials.html).
10. Boutin P. Total arthroplasty of the hip by fritted aluminum prosthesis. Experimental study and 1st clinical applications. *Rev Chir Orthop Reparatrice Appar Mot* 1972;58:229–246.
11. Hench L. Bioactive bone substitutes. In: Habal MB, Reddi AH, editors. *Bone Grafts and Graft Substitutes*. Philadelphia: W.B. Saunders; 1992, p. 263–275.
12. Jarcho M. Calcium phosphate ceramics as hard tissue prosthetics. *Clin Orthop Relat Res* 1981;157:259–278.
13. Tripathi G, Basu B. Injection molded HDPE-HA- $\text{Al}_2\text{O}_3$  hybrid composites for hard tissue replacement: mechanical, biological and protein adsorption behavior. *J Appl Polym Sci* 2011;124(3):2133–2143.
14. Tripathi G, Choudhury P, Basu B. Development of polymer based biocomposites: a review. *Mater Technol* 2010;25(3–4):158–176.
15. Nath S, Kalmudia S, Basu B. *In vitro* biocompatibility of novel biphasic calcium phosphate-mullite composites. *J Biomater Appl* 2013;27(5):497–509.
16. Martin RA, Jaffer Z, Tripathi G, Nath S, Mohanty M, FitzGerald V, Lagarde P, Flank A-M, Stamboulis A, Basu B. An X-ray micro-fluorescence study to investigate the distribution of Al, Si, P and Ca ions in the surrounding bone tissue after implantation of a hydroxyapatite-mullite ceramic composite in a rabbit animal model. *J Mater Sci* 2011;22:2537–2543.
17. Tripathi G, Dubey AK, Basu B. Evaluation of physico-mechanical properties and *in vitro* biocompatibility of compression molded HDPE based biocomposites with HA/ $\text{Al}_2\text{O}_3$  ceramic fillers and titanate coupling agents. *J Appl Polym Sci* 2011;124(4):3051–3063.
18. Nath S, Basu B, Mohanty M, Mohanan PV. *In vivo* response of novel hydroxyapatite-mullite composites: results up to 12 weeks of implantation. *J Biomed Mater Res Part B* 2009;90B:547–557.

19. Nath S, Bodhak S, Basu B. HDPE-Al<sub>2</sub>O<sub>3</sub>-HAp composites for biomedical applications: processing and characterization. *J Biomed Mater Res Part B Appl Biomater* 2009;88B: 1–11.
20. Basu B, Balani K. *Advanced Structural Ceramics*. Hoboken: Wiley; 2011.
21. Mixon M. Getting your nerve back: Dr. Christine Schmidt and her research team engineer ways to speed nerve regeneration and recovery after injury. [http://www.utexas.edu/features/2011/01/10/nerve\\_regeneration/](http://www.utexas.edu/features/2011/01/10/nerve_regeneration/).
22. Ahoki H. *Medical Applications for Hydroxyapatite*. St. Louis: Ishikayu Euro America; 1994.
23. Elliott JC. Structure and chemistry of the apatites and other calcium-orthophosphates. In: *Studios in Inorganic Chemistry 18*. Amsterdam: Elsevier; 1994.
24. Vallet-Regí M, Arcos D. Biomimetic nanoceramics in clinical use, *RSC. Nanosci Nanotechnol* 2008.
25. Wolff J. *The Law of Bone Remodeling*. Maquet R, Furlong R, (trans), Berlin: Springer-Verlag; 1986.
26. <http://www.orthosupersite.com/view.aspx?rid=26900>
27. Calandrelli L, Immirzi B, Malinconicon M, Luessenheide S, Passaro I, di Pasquale R, Oliva A. Natural and synthetic hydroxyapatite filled PCL: mechanical properties and biocompatibility analysis. *J Bioact Compat Polym* 2004;19:301–313.
28. Bronzino JD. *The Biomedical Engineering Handbook*. 2nd ed. Boca Raton, FL: CRC Press; 2000.
29. S.Sálcedo S, Arcos D, Vallet-Regí M. Upgrading calcium phosphate scaffolds for tissue engineering applications. *Key Eng Mater* 2008;377:19–42.
30. Gogolewski S. Bioresorbable polymers in trauma and bone surgery. *Injury* 2000;31 (Suppl 4):28–32.
31. Roy TD, Simon JL, Ricci JL, Rekow ED, Thompson VP, Parsons JR. Performance of degradable composite bone repair products made via three-dimensional fabrication techniques. *J Biomed Mater Res A* 2003;66(2):283–291.
32. Rokkanen P, Bostman O, Vainionpaa S, Makela EA, Hirvensalo E, Partio EK, et al. Absorbable devices in the fixation of fractures. *J Trauma* 1996;40(Suppl 3):S123–S127.
33. Coombes AG, Meikle MC. Resorbable synthetic polymers as replacements for bone graft. *Clin Mater* 1994;17(1):35–67.
34. Disegi JA, Eschbach L. Stainless steel in bone surgery. *Injury* 2000;31(Suppl 4):2–6.
35. Meaney DF. Mechanical properties of implantable biomaterials. *Clin Podiatr Med Surg* 1995;12(3):363–384.
36. Park HK, Dujovny M, Agner C, Diaz FG. Biomechanical properties of calvarium prosthesis. *Neurol Res* 2001;23(2–3):267–276.
37. Pohler OE. Unalloyed titanium for implants in bone surgery. *Injury* 2000;31(Suppl 4): 7–13.
38. Rah DK. Art of replacing craniofacial bone defects. *Yonsei Med J* 2000;41(6):756–765.
39. Berven S, Tay BK, Kleinstueck FS, Bradford DS. Clinical applications of bone graft substitutes in spine surgery: consideration of mineralized and demineralized preparations and growth factor supplementation. *Eur Spine J* 2001;10(Suppl 2):S169–S177.
40. Dard M, Sewing A, Meyer J, Verrier S, Roessler S, Scharnweber D. Tools for tissue engineering of mineralized oral structures. *Clin Oral Investig* 2000;4(2):126–129.



41. Hollinger JO, Seyfer AE. Bioactive factors and biosynthetic materials in bone grafting. *Clin Plast Surg* 1994;21(3):415–418.
42. Orban JM, Marra KG, Hollinger JO. Composition options for tissue-engineered bone. *Tissue Eng* 2002;8(4):529–539.
43. Zellin G, Hedner E, Linde A. Bone regeneration by a combination of osteopromotive membranes with different BMP preparations: a review. *Connect Tissue Res* 1996;35(1–4):279–284.
44. Warren SM, Nacamuli RK, Song HM, Longaker MT. Tissue-engineered bone using mesenchymal stem cells and a biodegradable scaffold. *J Craniofac Surg* 2004;15(1):34–37.
45. Noel D, Djouad F, Jorgense C. Regenerative medicine through mesenchymal stem cells for bone and cartilage repair. *Curr Opin Investig Drugs* 2002;3(7):1000–1004.
46. Leon CA. New perspectives in mercury porosimetry. *Adv Colloid Interface Sci* 1998;76–77:341–372.
47. Kuboki Y, Takita H, Kobayashi D, Tsuruga E, Inoue M, Murata M, et al. BMP-induced osteogenesis on the surface of hydroxyapatite with geometrically feasible and non-feasible structures: topology of osteogenesis. *J Biomed Mater Res* 1998;39(2):190–199.
48. Story BJ, Wagner WR, Gaisser DM, Cook SD, Rust-Dawicki AM. *In vivo* performance of a modified CSTi dental implant coating. *Int J Oral Maxillofac Implants* 1998;13(6):749–757.
49. Hulbert SF, Young FA, Mathews RS, Klawitter JJ, Talbert CD, Stelling FH. Potential of ceramic materials as permanently implantable skeletal prostheses. *J Biomed Mater Res* 1970;4(3):433–456.
50. Itala AI, Ylanen HO, Ekholm C, Karlsson KH, Aro HT. Pore diameter of more than 100 micron is not requisite for bone ingrowth in rabbits. *J Biomed Mater Res* 2001;58(6):679–683.
51. Ramakrishna S, Mayer J, Wintermantel E, Leong KW. Biomedical applications of polymer-composite materials: a review. *Compos Sci Technol* 2001;61:1189–1224.
52. Karageorgiou V, Kaplan D. Porosity of 3D biomaterial scaffolds and osteogenesis. *Biomaterials* 2005;26(27):5474–5491.
53. Chen Q, Roether JA, Boccaccini AR. Tissue engineering scaffolds from bioactive glass and composite materials. Ashammakhi N, Reis R, Chiellini F, editors. *Topics in Tissue Engineering*, vol. 4. 2008.
54. Wilson-Hench J. Osteoinduction. In: Williams DF, editor. *Progress in Biomedical Engineering*, vol 4. *Definitions in Biomaterials*. Amsterdam: Elsevier; 1987. p. 29.
55. Glantz PO. Comment. In: Williams DF, editor. *Progress in Biomedical Engineering*, vol 4. *Definitions in Biomaterials*. Amsterdam: Elsevier; 1987. p. 24.
56. Chang BS, Lee C-K, Hong K-S, Youn H-J, Ryu H-S, Chung S-S, Park K-W. Osteoconduction at porous hydroxyapatite with various pore configurations. *Biomaterials* 2000;21:1291–1298.
57. Ishaug-Riley SL, Crane-Kruger GM, Yaszemski MJ, Mikos AG. Three-dimensional culture of rat calvarial osteoblasts in porous biodegradable polymers. *Biomaterials* 1998;19:1405–1412.
58. Leong KF, Cheah CM, Chua CK. Solid freeform fabrication of three-dimensional scaffolds for engineering replacement tissues and organs. *Biomaterials* 2003;24:2363–2378.

59. Martin I, Padera RF, Vunjak-Novakovic G, Freed LE. *In vitro* differentiation of chick embryo bone marrow stromal cells into cartilaginous and bone-like tissues. *J Orthop Res* 1998;16:181–189.
60. Kuboki Y, Takita H, Kobayashi D, Tsuruga E, Inoue M, Murata M, et al. BMP-induced osteogenesis on the surface of hydroxyapatite with geometrically feasible and non-feasible structures: topology of osteogenesis. *J Biomed Mater Res* 1998;39(2):190–199.
61. Harvey EJ, Bobyn JD, Tanzer M, Stackpool GJ, Krygier JJ, Hacking SA. Effect of flexibility of the femoral stem on bone remodeling and fixation of the stem in a canine total hip arthroplasty model without cement. *J Bone Joint Surg Am* 1999;81(1):93–107.
62. Harvey EJ, Bobyn JD, Tanzer M, Stackpool GJ, Krygier JJ, Hacking SA. Effect of flexibility of the femoral stem on bone remodeling and fixation of the stem in a canine total hip arthroplasty model without cement. *J Bone Joint Surg Am* 1999;81(1):93–107.
63. Chang YS, Gu HO, Kobayashi M, Oka M. Influence of various structure treatments on histological fixation of titanium implants. *J Arthroplasty* 1998;13(7):816–825.
64. D Lima DD, Lemperle SM, Chen PC, Holmes RE, Colwell CWJr. Bone response to implant surface morphology. *J Arthroplasty* 1998;13(8):928–934.
65. Stefflik DE, Corpe RS, Young TR, Sisk AL, Parr GR. The biologic tissue responses to uncoated and coated implanted biomaterials. *Adv Dent Res* 1999;27–33.
66. Karageorgiou V, Kaplan D. Porosity of 3D biomaterial scaffolds and osteogenesis. *Biomaterials* 2005;26(27):5474–5491.
67. Simon JL, Roy TD, Parsons JR, Rekow ED, Thompson VP, Kemnitzer J, et al. Engineered cellular response to scaffold architecture in a rabbit trephine defect. *J Biomed Mater Res A* 2003;66(2):275–282.
68. Sachs EM, Haggerty JS, Cima MJ, Williams PA. Three-Dimensional Printing Techniques. US Patent No. 5,204,055. 1993.
69. Cima LG, Cima MJ. Preparation of Medical Devices by Solid Free-Form Fabrication Methods. US Patent No. 5,490,962. 1996.
70. Brecht JF. Binder Composition for use in Three Dimensional Printing. US Patent No. 5,851,465. 1998.
71. Brecht JF, Anderson TC, Russell DB. Three Dimensional Printing Material System and Method. US Patent No. 6,610,429. 2003.
72. Sachs EM. Powder Dispensing Apparatus Using Vibration. US Patent No. 6,036,777. 2000.
73. Brecht JF, Clark S, Gilchrist G. Three Dimensional Printing Material System and Method. US Patent No. 7,087,109. 2006.
74. Brecht JF, Anderson T. Method of Three Dimensional Printing. US Patent No. 5,902,441. 1999.
75. Cima M, Sachs E, Fan T, Brecht JF, Michaels SP, Khanuja S, Lauder A, Lee SJ, Brancazio D, Curodeau A, Tuerek H. Three-Dimensional Printing Techniques. US Patent No. 5,387,380. 1995.
76. Sachs EM, Haggerty JS, Cima MJ, Williams PA. Three-Dimensional Printing Techniques. US Patent No. 5,340,656. 1994.
77. Brecht JF, Anderson TC, Russell DB. Three Dimensional Printing Materials System. US Patent No. 6,416,850. 2002.

78. Schulman ML, Panzera C. Mass Production of Shells and Models for Dental Restorations Produced by Solid Free-Form Fabrication Methods. US Patent No. 6,821,462. 2004.
79. Lam CF, Mo XM, Teoh SH, Huttmacher DW. Scaffold development using 3D printing with a starch-based polymer. *Mater Sci Eng Part C* 2002;20:49–56.
80. Lee M, Dunn JC, Wu BM. Scaffold fabrication by indirect three-dimensional printing. *Biomaterials* 2005;26:4281–4289.
81. Giordano RA, Wu BM, Borland SW, Cima LG, Sachs EM, Cima MJ. Mechanical properties of dense polylactic acid structures fabricated by three-dimensional printing. *J Biomat Sci Polym* 1996;E8:63–75.
82. Boland ED, Matthews JA, Pawlowski KJ, Simpson DG, Wnek GE, Bowlin GL. Electrospinning collagen and elastin: preliminary vascular tissue engineering. *Front Biosci* 2004;9:1422–1432.
83. Sell SA, McClure MJ, Garg K, Wolfe PS, Bowlin GL. Electrospinning of collagen/biopolymers for regenerative medicine and cardiovascular tissue engineering. *Adv Drug Deliv Rev* 2009;61:1007–1019.
84. McClure MJ, Sell SA, Simpson DG, Walpoth BH, Bowlin GL. A three-layered electrospun matrix to mimic native arterial architecture using polycaprolactone, elastin, and collagen: a preliminary study. *Acta Biomater* 2011;6:2422–2433.
85. Baker SC, Atkin N, Gunning PA, Granville N, Wilson K, Wilson D, Southgate J. Characterization of polystyrene scaffolds for three-dimensional *in vitro* biological studies. *Biomaterials* 2006;27:3136–3146.
86. Chen DC, Avansino JR, Agopian VG, Hoagland VD, Woolman JD, Pan S, Ratner BD, Stelzner M. Comparison of polyester scaffolds for bioengineered intestinal mucosa. *Cells Tissues Organs* 2006;184:154–165.
87. Brizzola S, de Eguileor M, Brevini T, Grimaldi A, Congiu T, Neuenschwander P, Acocella F. Morphologic features of biocompatibility and neoangiogenesis onto a biodegradable tracheal prosthesis in an animal model. *Interact Cardiovasc Thorac Surg* 2009;8:610–614.
88. Leong MF, Chian KS, Mhaisalkar PS, Ong WF, Ratner BD. Effect of electrospun poly (D,L-lactide) fibrous scaffold with nanoporous surface on attachment of porcine esophageal epithelial cells and protein adsorption. *J Biomed Mater Res A* 2009;89:1040–1048.
89. Mano JF, Silva GA, Azevedo HS, Malafaya PB, Sousa RA, Silva SS, Boesel LF, Oliveira JM, Santos TC, Marques AP, Neves NM, Reis RL. Natural origin biodegradable systems in tissue engineering and regenerative medicine: present status and some moving trends. *J R Soc Interface* 2007;4:999–1030.
90. Young AC, Omatete OO, Janney MA, Menchhofer PA. Gelcasting of alumina. *J Am Ceram Soc* 1991;74:612–618.
91. Nunn SD, Kirby GH. Green machining of gelcast ceramic materials. *Ceram Eng Sci Proc* 1996;17:209–213.
92. Leong KF, Cheah CM, Chua CK. Solid freeform fabrication of three-dimensional scaffolds for engineering replacement tissues and organs. *Biomaterials* 2003;24:2363–2378.
93. Yang S, Leong KF, Du Z, Chua CK. The design of scaffolds for use in tissue engineering. Part I. Traditional factors. *Tissue Eng* 2001;7:679–689.

94. Barralet JE, Grover L, Gaunt T, Wright AJ, Gibson IR. Preparation of macroporous calcium phosphate cement tissue engineering scaffold. *Biomaterials* 2002;23(15):3063–3072.
95. Borden M, El-Amin SF, Attawia M, Laurencin CT. Structural and human cellular assessment of a novel microsphere-based tissue engineered scaffold for bone repair. *Biomaterials* 2003;24(4):597–609.
96. Lin AS, Barrows TH, Cartmell SH, Guldborg RE. Micro architectural and mechanical characterization of oriented porous polymer scaffolds. *Biomaterials* 2003;24(3):481–489.
97. Burdick JA, Padera RF, Huang JV, Anseth KS. An investigation of the cytotoxicity and histocompatibility of *in situ* forming lactic acid based orthopedic biomaterials. *J Biomed Mater Res* 2002;63(5):484–491.
98. Burdick JA, Frankel D, Dernel WS, Anseth KS. An initial investigation of photocurable three-dimensional lactic acid based scaffolds in a critical-sized cranial defect. *Biomaterials* 2003;24(9):1613–1620.
99. Story BJ, Wagner WR, Gaisser DM, Cook SD, Rust-Dawicki AM. *In vivo* performance of a modified CSTi dental implant coating. *Int J Oral Maxillofac Implants* 1998;13(6):749–757.
100. Koça N, Timuçina M, Korkusuzb F. Fabrication and characterization of porous tricalcium phosphate ceramics. *Ceram Int* 2004;30:205–211.
101. Li SH, de Wijn JR, Layrolle P, de Groot K. Novel method to manufacture porous hydroxyapatite by dual-phase mixing. *J Am Ceram Soc* 2003;86(1):65–72.
102. Tang YJ, Tang YF, Lv CT, Zhou ZH. Preparation of uniform porous hydroxyapatite biomaterials by a new method. *Appl Surf Sci* 2008;254:5359–5362.
103. Itatani K, Uchino T, Okada I. Preparation of porous hydroxyapatite ceramics from hollow spherical agglomerates using a foaming agent of H<sub>2</sub>O<sub>2</sub>. *J Soc Inorg Mater Jap* 2003;10(306):308–315.
104. Thijs I, Luyten J, Mullens S. Producing ceramic foams with hollow spheres. *J Am Ceram Soc* 2003;87(1):170–172.
105. Ramay HR, Zhang M. Preparation of porous hydroxyapatite scaffolds by combination of the gel-casting and polymer sponge methods. *Biomaterials* 2003;24:3293.
106. Sopyan I, Mel M, Ramesh S, Khalid KA. Porous hydroxyapatite for artificial bone. *Sci Technol Adv Mater* 2007;8:116–123.
107. Tripathi G, Basu B. A porous hydroxyapatite scaffold for bone tissue engineering: physico-mechanical and biological evaluations. *Ceram Int* 2012;(38):341–349.
108. Kwon S-H, Jun Y-K, Hong S-H, Lee I-S, Kim H-E. Calcium phosphate bioceramics with various porosities and dissolution rate. *J Am Ceram Soc* 2002;85(12):3129–3131.
109. Gervaso F, Scalera F, Padmanabhan SK, Sannino A, Licciulli A. High-performance hydroxyapatite scaffolds for bone tissue engineering applications. *Int J Appl Ceram Technol* 2011;1–10.
110. Schwartzwalder K, Sommers AV. Method of Making Porous Ceramic Articles. US Patent No. 3090094. 1963.
111. Zhu X, Jiang D, Tan S. The control of slurry rheology in the processing of reticulate porous ceramics. *Mater Res Bull* 2002;37:541–553.
112. Pu X, Liu X, Qiu F, Huang L. Novel method to optimize the structure of reticulated porous ceramics. *J Am Ceram Soc* 2004;87(7):1392–1394.

113. Lin K, Chang J, Zeng Y, Qian W. Preparation of macroporous calcium silicate ceramics. *Mater Lett* 2004;58:2109–2113.
114. Huang X, Miao X. Novel porous hydroxyapatite prepared by combining H<sub>2</sub>O<sub>2</sub> foaming with PU sponge and modified with PLGA and bioactive glass. *J Biomater Appl* 2007;21(4):351–374.
115. Narbat MK, Orang F, Hashtjin MS, Goudarzi A. Fabrication of porous hydroxyapatite-gelatin composite scaffolds for bone tissue engineering. *Iran Biomed J* 2006;10(4):215–223.
116. Lyckfeldt O, Ferreira JMF. Processing of porous ceramics by starch consolidation. *J Eur Ceram Soc* 1998;18:131–140.
117. Deville S, Saiz E, Tomsia A. Freeze casting of hydroxyapatite scaffolds for bone tissue engineering. *Biomaterials* 2006;27:5480–5489.
118. Potoczek M. Hydroxyapatite foams produced by gelcasting using agarose. *Mater Lett* 2008;62:1055–1057.
119. Giordano RA, Wu BM, Borland SW, Cima LG, Sachs EM, Cima MJ. Mechanical properties of dense polylactic acid structures fabricated by three dimensional printing. *J Biomater Sci Polym Ed* 1996;8(1):63.
120. Kim SS, Utsunomiya H, Koski JA, Wu BM, Cima MJ, Sohn J, Mukai K, Griffith LG, Vacanti JP. *Ann Surg* 1998;228(1):8.
121. Mann S, Webb J, Williams RJP. *Biom mineralization: Chemical and Biochemical Perspectives*. New York: VCH Publishers; 1989.
122. Deville S, Saiz E, Tomsia A. Freeze casting of hydroxyapatite scaffolds for bone tissue engineering. *Biomaterials* 2006;27:5480–5489.
123. Deville S, Saiz E, Nalla RK, Tomsia A. Freezing as a path to build complex composites. *Science* 2006;311:515–518.
124. Fu Q, Rahaman MN, Dogan F, Bal BS. Freeze casting of porous hydroxyapatite scaffolds. II. Sintering, microstructure, and mechanical behavior. *J Biomed Mater Res Part B Appl Biomater* 2008;86B:514–522.
125. Chu TM, Orton DG, Hollister SJ, Feinberg SE, Halloran JW. Mechanical and *in vivo* performance of hydroxyapatite implants with controlled architectures. *Biomaterials* 2002;23(5):1283–1293.
126. Kim HW, Knowles JC, Kim HE. Hydroxyapatite/poly( $\epsilon$ -caprolactone) composite coatings on hydroxyapatite porous bone scaffold for drug delivery. *Biomaterials* 2004;25(7–8):1279–1287.
127. Veiga DD, Antunes JC, Gómez RG, Mano JF, Ribelles JLG, Soria JM. Three-dimensional scaffolds as a model system for neural and endothelial “*in vitro*” culture. *J Biomater Appl* 2008;22:293.
128. Kim HW, Knowles JC, Kim HE. Hydroxyapatite porous scaffold engineered with biological polymer hybrid coating for antibiotic vancomycin release. *J Mater Sci Mater Med* 2005;16:189–195.
129. Callcut S, Knowles JC. Correlation between structure and compressive strength in a reticulate glass-reinforced hydroxyapatite foam. *J Mater Sci Mater Med* 2002;13:485–489.
130. Stephan TB, Hendrik B, Oliver K, Hermann S, Timothy D, Sureshan S, Jörg W, Eugene S, Patrick HW. Endocultivation: 3D printed customized porous scaffolds for heterotopic bone induction. *Oral Oncology* 2009;45:e181–e188.

131. Chen QZ, Thompson ID, Boccaccini AR. 45S5 Bioglass1-derived glass-ceramic scaffold for bone tissue engineering. *Biomaterials* 2006;27:2414–2425.
132. Tsuruga E, Takita H, Itoh H, Wakisaka Y, Kuboki Y. Pore size of porous hydroxyapatite as the cell-substratum controls BMP-induced osteogenesis. *J Biochem-Tokyo* 1997;121(2):317–324.
133. Teixeira S, Rodriguez MA, Pena P, De Aza AH, De Aza S, Ferraz MP, Monteiro FJ. Physical characterization of hydroxyapatite porous scaffolds for tissue engineering. *Mater Sci Eng C* 2009;29:1510–151.
134. Barralet JE, Grover L, Gaunt T, Wright AJ, Gibson IR. Preparation of macroporous calcium phosphate cement tissue engineering scaffold. *Biomaterials* 2002;23(15):3063–3072.
135. Wu C, Chang J, Zhai W, Ni S, Wang J. Porous akermanite scaffolds for bone tissue engineering: preparation, characterization, and *in vitro* studies. *J Biomed Mater Res B Appl Biomater* 2006;78:47–55.
136. Zhao J, Lu X, Duan K, Guo LY, Zhou SB, Weng J. Improving mechanical and biological properties of macroporous HA scaffolds through composite coatings. *Colloids Surf B Biointerfaces* 2009;74:159–166.
137. Woodard JR, Hilldore AJ, Lan SK, Park CJ, Morgan AW, Eurell JAC, Clark SG, Wheeler MB, Jamison RD, Johnson AJ. The mechanical properties and osteoconductivity of hydroxyapatite bone scaffolds with multi-scale porosity. *Biomaterials* 2007;28:45–54.
138. Sepulveda P, Ortega FS, Innocentini MDM, Pandolfelli VC. Properties of highly porous hydroxyapatite obtained by the gelcasting of foams. *J Am Ceram Soc* 2000;83:3021–3024.
139. Kim HW, Knowles JC, Kim HE. Hydroxyapatite porous scaffold engineered with biological polymer hybrid coating for antibiotic vancomycin release. *Sci Mater Med* 2005;16:189–195.
140. Fu Q, Rahaman MN, Bal BS, Huang W, Day DE. Preparation and bioactive characterization of a porous 13-93 glass, and fabrication into the articulating surface of a proximal tibia. *J Biomed Mater Res A* 2007;82:222–229.
141. Cyster LA, Grang DM, Howdle SM, Rose FRAJ, Irvine DJ, Freeman D, Scotchfor CA, Shakesheff KM. The influence of dispersant concentration on the pore morphology of hydroxyapatite ceramics for bone tissue engineering. *Biomaterials* 2005;26:697–702.
142. Harris LD, Kim BS, Mooney DJ. Open pore biodegradable matrices formed with gas foaming. *J Biomed Mater Res* 1998;42:396–402.
143. Dong Z, Li Y, Zou Q. Degradation and biocompatibility of porous nano-hydroxyapatite/polyurethane composite scaffold for bone tissue engineering. *Appl Surf Soc* 2009;255:6087–6091.
144. Zhang C, Wang J, Feng H, Lu B, Song Z, Zhang X. Replacement of segmental bone defects using porous bioceramic cylinders: a biomechanical and X-ray diffraction study. *J Biomed Mater Res* 2001;54(3):407–411.
145. Karageorgiou V, Kaplan D. Porosity of 3D biomaterial scaffolds and osteogenesis. *Biomaterials* 2005;26:5474–5491.
146. Kima H-M, Himeno T, Kokubo T, Nakamura T. Process and kinetics of bonelike apatite formation on sintered hydroxyapatite in a simulated body fluid. *Biomaterials* 2005;26:4366–4373.
147. Tas AC. Synthesis of biomimetic Ca-hydroxyapatite powders at 37 °C in synthetic body fluids. *Biomaterials* 2000;21:1429–1438.

148. Guo H, Su J, Wei J, Kong H, Liu C. Biocompatibility and osteogenicity of degradable Ca-deficient hydroxyapatite scaffolds from calcium phosphate cement for bone tissue engineering. *Acta Biomater* 2009;5:268–278.
149. Park A, Wu B, Griffith LG. Integration of surface modification and 3D fabrication techniques to prepare patterned poly(L-lactide) substrates allowing regionally selective cell adhesion. *J Biomater Sci Polym Ed* 1998;9:89.
150. Peng Q, Jiang F, Huang P, Zhou S, Weng J, Bao C, Zhang C, Yu H. A novel porous bioceramics scaffold by accumulating hydroxyapatite spherules for large bone tissue engineering *in vivo*. I. Preparation and characterization of scaffold. *J Biomed Mater Res* 2010;93A:920–929.
151. Becker ST, Bolte H, Krapf O, Seitz H, Douglas T, Sivananthan S, Wiltfang J, Sherry E, Warnke PH. Endocultivation: 3D printed customized porous scaffolds for heterotopic bone induction. *Oral Oncol* 2009;45:e181–e188.
152. Tripathi G, Basu B. Processing and biological evaluation of porous HA/poly(methyl methacrylate) hybrid composite. *Int J Adv Eng Sci Appl Math* 2010;2(4):161–167.
153. Ma PX, Zhang R, Xiao G, Franceschi R. Engineering new bone tissue *in vitro* on highly porous poly(alpha-hydroxyl acids)/hydroxyapatite composite scaffolds. *J Biomed Mater Res* 2001;54(2):284–293.
154. Ramirez PA, Romito A, Cosentino F, Milella, E. The influence of titania/hydroxyapatite composite coatings on *in vitro* osteoblasts behaviour. *Biomaterials* 2001;22(12):1467–1474.
155. Kwon SH, Jun YK, Hong SH, Lee IS, Kim HE. Calcium phosphate bioceramics with various porosities and dissolution rate. *J Am Ceram Soc* 2002;85(12):3129–3131.